[AMERICAN JOURNAL OF SCIENCE, VOL. 295, MARCH, 1995, P. 245–281]

American Journal of Science

*MARCH 1995*

# A CHEMICAL AND THERMODYNAMIC MODEL OF DIOCTAHEDRAL 2:1 LAYER CLAY MINERALS IN DIAGENETIC PROCESSES: DEHYDRATION OF DIOCTAHEDRAL ALUMINOUS SMECTITE AS A FUNCTION OF TEMPERATURE AND DEPTH IN SEDIMENTARY BASINS

BARBARA RANSOM* and HAROLD C. HELGESON
Department of Geology and Geophysics,
University of California, Berkeley, California 94720

**ABSTRACT. The standard molal thermodynamic properties of dehydration of dioctahedral aluminous smectites have been computed for temperatures to 300 °C and pressures to 5 kb.[1] By combining values of the standard molal Gibbs free energies of the dehydration reaction at 25 °C and 1 bar (Ransom and Helgeson, 1994a) with those of the standard molal entropy, heat capacity, and volume of dehydration generated from the thermodynamic properties of interlayer and bulk $H_2O$ (Ransom and Helgeson, 1994b; Johnson and Norton, 1991), the equilibrium hydration states of dioctahedral aluminous smectites can be predicted as a function of temperature and pressure in geologic systems. Calculations of this kind indicate that smectite gradually dehydrates with increasing temperature and burial depth. Combining the results of such calculations with equations that take into account the fact that smectites in nature contain more than one type of interlayer cation make it possible to estimate the amount of interlayer $H_2O$ released to pore spaces as smectites are buried along crustal geotherms. Calculations indicate that at 100 °C and 3.5 km along US Gulf Coast geotherms, smectites contain ~15 to 65 percent less interlayer $H_2O$ than when they were deposited, depending on the interlayer cations present. Calculations also indicate that with increasing burial monovalent cations are increasingly preferred over divalent cations in smectite interlayers, a trend verified by transmission electron microscope studies (Ahn and Peacor, 1986). Calculation of reaction properties indicate that both the volume and enthalpy of smectite dehydration are positive along crustal geotherms. For geologic systems for which the volume change is suppressed, a sudden pressure release such as failure along a fault could trigger rapid smectite dehydration resulting in an episode**

* Present address: Scripps Institution of Oceanography, Geological Research Division 0220, La Jolla, California 92093.

[1] The term dehydration is used in the present communication to refer to the loss of intracrystalline interlayer $H_2O$ from smectite. Thermodynamically, smectite dehydration can be represented as a regular solid solution of homologous hydrous and anhydrous thermodynamic components (Ransom and Helgeson, 1994a). The terms hydrous and anhydrous refer to chemical or physical units with and without interlayer $H_2O$, respectively.

**of rapid fluid generation accompanied by a short term depression of the local geothermal gradient.**

## INTRODUCTION

It has long been postulated that intracrystalline $H_2O$ expelled from smectite interlayers plays a significant role in diagenetic processes. Nevertheless, the actual amount of interlayer $H_2O$ released during sediment burial and diagenesis is still a matter of controversy. Recent calculation of regular solution Margules parameters and standard molal Gibbs free energies of dehydration for dioctahedral aluminous smectites at 25 °C and 1 bar (Ransom and Helgeson, 1994a), together with estimates of the standard molal heat capacity, entropy, and volume of interlayer $H_2O$ retrieved from calorimetric and density data reported in the literature (Ransom and Helgeson, 1994b), permit calculation of the equilibrium hydration state of smectite as a function of temperature and pressure. The purpose of the present communication is to report the results of such calculations and to predict the extent and consequences of smectite dehydration as a function of depth in sedimentary basins.

Smectite dehydration has been linked to phenomena as diverse as sediment overpressuring (Powers, 1967; Barker, 1972; Magara, 1975; Plumley, 1980; Bethke, 1986), the migration of petroleum (Powers, 1967; Burst, 1969; Bruce, 1984), listric faulting (Bruce, 1984), and what is commonly referred to as the "smectite to illite transition"[2] (Powers, 1967; Perry and Hower, 1972; Weaver and Beck, 1971, Hower and others, 1976; Freed and Peacor, 1989; Pytte and Reynolds, 1988; Velde and Vasseur, 1992; and others). However, its actual role in these processes is difficult to assess, because the extent to which smectite dehydrates with increasing burial has yet to be measured *in situ*.

Over the years, laboratory studies have been performed at elevated temperatures and pressures and various ionic strengths in phenomenological attempts to duplicate the dehydration of smectite during burial and diagenesis (Khitarov and Pugin, 1966; Bird, 1984; Koster van Groos and Guggenheim, 1984, 1986, 1987; Colten, 1986; Hall, Astill, and McConnell, 1986; Colten-Bradley, 1987; Huang, Bassett, and Wu, 1994). However, these experiments have been hampered by uncertainties arising from rapid heating rates, the application of hydrostatic rather than nonhydrostatic stress, insufficient proof that long term steady states were achieved, and differences between laboratory and natural samples. Similarly, although Reynolds (1992) has shown that the expandabilities of ethylene glycol-treated clay samples are not significantly affected by different sample preparation techniques, the relevance of these expandabilities to the hydration state of smectites in geologic systems remains

[2] From a thermodynamic and petrologic point of view, the phrase "smectite to illite transition" is a misnomer because it implies a polymorphic phase transition. Such a transition requires the composition of the minerals to be the same before and after the transition. Because the minerals smectite and illite have distinctly different compositions (Ransom and Helgeson, 1993), there can be no such transition between them.

questionable to the extent that this expandability differs from that of $H_2O$-saturated smectites in natural environments. An alternate approach involves characterizing the equilibrium phase relations in the system and using thermodynamic calculations to assess the relative importance of the various chemical and physical parameters that affect smectite dehydration under burial conditions. Such calculations can then be used to make predictions of the equilibrium hydration state of smectite as a function of temperature and pressure along crustal geotherms. These results can then be compared with field observations of sediment compaction and overpressuring and used to facilitate the design of field sampling programs and geologically relevant experiments.

GLOSSARY OF SYMBOLS

| | |
|---|---|
| $a_{as}$, $a_{hs}$ | Activity of anhydrous and hydrous components, respectively, of smectite solid solutions. |
| $a_{Ca(as)}$, $a_{Ca(hs)}$ | Activity of anhydrous and hydrous Ca-smectite components, respectively. |
| $a_{H_2O}$ | Activity of $H_2O$ relative to the liquid standard state. |
| $a_{Na(as)}$, $a_{Na(hs)}$ | Activity of anhydrous and hydrous Na-smectite components, respectively. |
| as | Symbolic representation of anhydrous components of smectite solid solutions. |
| $C^\circ_{P_r,as}$, $C^\circ_{P_r,hs}$ | Standard molal heat capacity at 1 bar of anhydrous and hydrous smectite components, respectively. |
| $C^\circ_{P_r,H_2O}$, $C^\circ_{P_r,H_2O(il)}$ | Standard molal heat capacity at 1 bar of bulk and interlayer $H_2O$, respectively. |
| $\delta C^\circ_{P_r,s}$ | Difference between the standard molal heat capacity of hydrous and anhydrous components of smectite solid solutions at 1 bar (eq A.9 in app. A). |
| $\Delta C^\circ_{P,r}$, $\Delta C^\circ_{P_r,r}$ | Standard molal heat capacity of reaction and that of reaction at 1 bar, respectively. |
| $G^\circ_{H_2O}$ | Standard molal Gibbs free energy of bulk $H_2O$. |
| $\delta G^\circ_{f,s,P_r,T_r}$ | Difference between the standard molal Gibbs free energy of formation from the elements at 1 bar and 25 °C of hydrous and anhydrous components of smectite solid solutions (eq B.11 in app. B). |
| $\Delta G^\circ_{f,as,P_r,T_r}$, $\Delta G^\circ_{f,hs,P_r,T_r}$, $\Delta G^\circ_{f,H_2O,P_r,T_r}$ | Standard molal Gibbs free energy of formation from the elements of anhydrous and hydrous smectite components, respectively, and that of bulk water at 1 bar and 25 °C. |
| $\Delta G^\circ_r$ | Standard molal Gibbs free energy of reaction. |
| hs | Symbolic representation of the hydrous components of smectite solid solutions. |
| $H_2O$(il) | Intracrystalline interlayer $H_2O$ in smectite. |

$H^\circ_{H_2O}$ Standard molal enthalpy of bulk $H_2O$.

$\delta H^\circ_{f,s,P_r,T_r}$ Difference between the standard molal enthalpy of formation from the elements at 1 bar and 25 °C of anhydrous and hydrous components of smectite solid solutions (eq B.9 in app. B).

$\Delta H^\circ_{f,as,P_r,T_r}$, $\Delta H^\circ_{f,hs,P_r,T_r}$, $\Delta H^\circ_{f,H_2O,P_r,T_r}$, $\Delta H^\circ_{f,H_2O(il),P_r,T_r}$ Standard molal enthalpy of formation from the elements of anhydrous and hydrous smectite components, that of bulk $H_2O$ and that of interlayer $H_2O$, respectively, at 25 °C and 1 bar.

$\Delta H^\circ_r$ Standard molal enthalpy of reaction.

K Equilibrium constant.

$k_{0,H_2O(il)}$, $k_{1,H_2O(il)}$, $k_{2,H_2O(il)}$, $k_{3,H_2O(il)}$ Berman-Brown (Berman and Brown, 1985) heat capacity power function coefficients for interlayer $H_2O$.

$n_c$ Number of moles of interlayer $H_2O$.

P, $P_r$ Pressure in bars and the reference pressure (1 bar).

R Gas constant (1.9872 cal $mol^{-1}$ $K^{-1}$).

$S^\circ_{as,P_r,T_r}$, $S^\circ_{hs,P_r,T_r}$ Standard molal entropy at 1 bar and 25 °C of anhydrous and hydrous components, respectively, of smectite solid solutions.

$S^\circ_{H_2,P_r,T_r}$ Standard molal entropy of hydrogen gas at 1 bar and 25 °C.

$S^\circ_{H_2O}$, $S^\circ_{H_2O(il)}$ Standard molal entropy of bulk and interlayer $H_2O$, respectively.

$S^\circ_{O_2,P_r,T_r}$ Standard molal entropy of oxygen gas at 1 bar and 25 °C.

$\delta S^\circ_{s,P_r,T_r}$, $\delta S^\circ_{f,s,P_r,T_r}$ Difference between the standard molal entropy at 1 bar and 25 °C and that of formation from the elements, respectively, of hydrous and anhydrous components of smectite solid solutions (eq A.2 in app. A and eq B.12 in app. B, respectively).

$\Delta S^\circ_{f,as,P_r,T_r}$, $\Delta S^\circ_{f,hs,P_r,T_r}$ Standard molal entropy of formation from the elements at 1 bar and 25 °C of anhydrous and hydrous components, respectively, of smectite solid solutions.

$\Delta S^\circ_r$ Standard molal entropy of reaction.

T, $T_r$ Temperature in Kelvin and the reference temperature (298.15 K), respectively.

$V^\circ_{as,P_r,T_r}$, $V^\circ_{hs,P_r,T_r}$ Standard molal volume of the anhydrous and hydrous components of smectite solid solutions, respectively, at 1 bar and 25 °C.

$V^\circ_{H_2O}$, $V^\circ_{H_2O(il)}$ Standard molal volume of bulk and interlayer $H_2O$, respectively.

$\delta V^\circ_{s,P_r,T_r}$ Difference between the standard molal volume of hydrous and anhydrous components of smectite solid solutions in (eq A.3 in app. A).

$\Delta V_r^\circ$ Standard molal volume of reaction.

$W_{Ca}$, $W_{Na}$ Temperature-pressure-independent Margules parameter of Ca- and Na-smectite components, respectively, in (Na, Ca)-smectite solid solutions.

$W_s$ Temperature-pressure-independent Margules parameter for a binary regular solid solution of hydrous and anhydrous smectite components.

$X_a$ Mole fraction of anhydrous components in smectite.

$X_{as}$, $X_{hs}$ Mole fraction of anhydrous and hydrous smectite components, respectively.

$X_{Ca}$, $X_{Na}$ Mole fraction of Ca-smectite and Na-smectite components, respectively.

$X_{Ca(as)}$, $X_{Ca(hs)}$ Mole fraction of anhydrous and hydrous Ca-smectite components, respectively.

$X_h$ Mole fraction of hydrous components in smectite.

$X_{Na(as)}$, $X_{Na(hs)}$ Mole fraction of anhydrous and hydrous Na-smectite components, respectively.

$\lambda_{as}$, $\lambda_{hs}$ Activity coefficient of anhydrous and hydrous components, respectively, of smectite solid solutions.

$\lambda_{Ca(as)}$, $\lambda_{Ca(hs)}$ Activity coefficient of anhydrous and hydrous Ca-smectite components, respectively, of smectite solid solutions.

$\lambda_{Na(as)}$, $\lambda_{Na(hs)}$ Activity coefficient of anhydrous and hydrous Na-smectite components, respectively, of smectite solid solutions.

## CALCULATION OF THE STANDARD MOLAL GIBBS FREE ENERGIES OF REACTION AND EQUILIBRIUM CONSTANTS FOR SMECTITE DEHYDRATION AS A FUNCTION OF TEMPERATURE AND PRESSURE TO 300 °C AND 5 KB

Following Ransom and Helgeson (1993, 1994a), the dehydration of smectite can be described symbolically in terms of homologous hydrous (hs) and anhydrous (as) components[3] by writing

$$hs \rightleftarrows as + n_c H_2O \qquad (1)$$

where $n_c$ stands for the number of moles of $H_2O$ evolved in the reaction. This value is 4.5 for smectite components with stoichiometries written in terms of a half unit cell: $O_{10}(OH)_2$ (Ransom and Helgeson, 1994a). Definitions of the symbols in reaction (1), as well as those in the equations below are listed in the Glossary.

[3] The term component is used in this communication in its strict thermodynamic sense. A thermodynamic component of a mineral corresponds to a chemical formula unit representing one of the minimum number of independent variables required to describe the composition of the mineral. All stoichiometric minerals are thus composed of a single component corresponding to the formula of the mineral. However, because the term component has no necessary physical connotation, the minerals themselves are not components.

The law of mass action for reaction (1) can be written as

$$K = \frac{a_{as}(a_{H_2O})^{n_c}}{a_{hs}} \tag{2}$$

where K represents the equilibrium constant, $a_{H_2O}$ refers to the activity of $H_2O$, and $a_{hs}$ and $a_{as}$ denote the activities of the hydrous and anhydrous components of the solid solution, respectively.[4] These activities can be expressed in terms of the mole fractions ($X_{hs}$ and $X_{as}$) and activity coefficients ($\lambda_{hs}$ and $\lambda_{as}$) of the components by taking account of

$$a_{hs} = X_{hs}\lambda_{hs} \tag{3}$$

and

$$a_{as} = X_{as}\lambda_{as}. \tag{4}$$

Combining eqs (2) to (4) leads to

$$K = \frac{X_{as}\lambda_{as}(a_{H_2O})^{n_c}}{X_{hs}\lambda_{hs}}. \tag{5}$$

For a binary system, the logarithmic analog of eq (5) can be combined with

$$X_{as} = 1 - X_{hs} \tag{6}$$

to give

$$\log K = \log\left(\frac{1 - X_{hs}}{X_{hs}}\right) + \log\left(\frac{\lambda_{as}}{\lambda_{hs}}\right) + n_c \log a_{H_2O}. \tag{7}$$

Consideration of experimental data indicates that solid solutions of homologous hydrous and anhydrous smectite components at 25 °C and 1 bar are consistent with regular solution theory (Ransom and Helgeson, 1994a) which permits eq (7) to be written for unit activity of $H_2O$ as

$$\log K = \log\left(\frac{1 - X_{hs}}{X_{hs}}\right) + \frac{W_s(2X_{hs} - 1)}{2.303\ RT} \tag{8}$$

where $W_s$ stands for the regular solution Margules parameter, R refers to the gas constant, and T denotes temperature in Kelvin. Values of $W_s$ for dioctahedral aluminous smectites were derived by Ransom and Helgeson (1994a) and are shown in table 1.

[4] The standard state for minerals and water adopted in the present study is one of unit activity of the pure solid or liquid at any pressure and temperature. The standard state for gases calls for unit fugacity of the hypothetical ideal gas at 1 bar and any temperature.

TABLE 1

*Calculated Margules parameters ($W_s$), $\Delta G^\circ_{r,P_r,T_r}$ and log K for the dehydration of various homologous homoionic smectite solid solutions at 25 °C and 1 bar in accord with reaction (1)*

| Smectite* | $W_S$ kcal mol$^{-1}$ | $\Delta G^\circ_{r,Pr,Tr}$ kcal mol$^{-1}$ | log K |
|---|---|---|---|
| Na-smectite | - 3.254 | 1.047 | - 0.767 |
| K-smectite | - 3.289 | 0.207 | - 0.151 |
| $NH_4$-smectite | - 3.293 | 0.129 | - 0.095 |
| Rb-smectite | - 3.300 | - 0.052 | 0.038 |
| Cs-smectite | - 3.314 | - 0.374 | 0.274 |
| Mg-smectite | - 2.806 | 5.842 | - 4.28 |
| Ca-smectite | - 2.883 | 4.926 | - 3.61 |
| Sr-smectite | - 2.909 | 4.620 | - 3.39 |
| Ba-smectite | - 2.948 | 4.160 | - 3.05 |

* The stoichiometries of the components of the binary smectite solid solutions listed here are given in Ransom and Helgeson (1994a) as are the values of $W_s$ and $\Delta G^\circ_{r,P_r,T_r}$.

The equilibrium constant is related to the standard molal Gibbs free energy of reaction (1) at any temperature and pressure ($\Delta G^\circ_r$) by

$$\log K = -\frac{\Delta G^\circ_r}{2.303\ RT}. \tag{9}$$

The temperature and pressure dependence of $\Delta G^\circ_r$ can be expressed as

$$\Delta G^\circ_r = \Delta G^\circ_{r,P_r,T_r} - \Delta S^\circ_{r,P_r,T_r}(T - T_r) + \int_{T_r}^{T} \Delta C^\circ_{P_r,r}\, dT - T\int_{T_r}^{T} \Delta C^\circ_{P_r,r}\, d\ln T + \int_{P_r}^{P} \Delta V^\circ_r\, dP \tag{10}$$

where $T_r$ and $P_r$ stand for the reference temperature (298.15 K) and pressure (1 bar), and $\Delta G^\circ_{r,P_r,T_r}$, $\Delta S^\circ_{r,P_r,T_r}$, $\Delta C^\circ_{P_r,r}$, and $\Delta V^\circ_r$ represent the standard molal Gibbs free energy, entropy, heat capacity, and volume of reaction (1) at the reference temperature and pressure or those of interest, as indicated by the subscripts or lack thereof, respectively.

Values of $\Delta G^\circ_{r,P_r,T_r}$ required to evaluate eq (10) are given by Ransom and Helgeson (1994a) for smectites with various interlayer cations. These values are provided in table 1, together with corresponding values of log K computed from eq (9). Algorithms for calculating $\Delta S^\circ_{r,P_r,T_r}$, $\Delta C^\circ_{P_r,r}$, and $\int_{P_r}^{P} \Delta V^\circ_r\, dP$ in eq (10) are described in app. A (eqs A.4, A.8, and A.12). These algorithms were solved using the thermodynamic properties of

TABLE 2

*Estimated values of the standard molal entropy, volume, and heat capacity of interlayer $H_2O$ in smectite at 25 °C and 1 bar, taken from Ransom and Helgeson (1994b), in addition to Berman-Brown and compatible Maier-Kelley heat capacity power function coefficients for interlayer $H_2O$*

| Entropy cal mol$^{-1}$ K$^{-1}$ | Volume cm$^3$ mol$^{-1}$ | Heat Capacity cal mol$^{-1}$ |
|---|---|---|
| 13.15 | 17.22 | 11.46 |
| **Berman-Brown*** | | |
| $C_P^\circ = k_0 + k_1T^{-0.5} + k_2T^{-2} + k_3T^{-3}$ | | |
| $k_0$ | $k_1\times10^{-2}$ | $k_2\times10^{-3}$ | $k_2\times10^{-7}$ |
| 31.481 | - 3.796 | 0.0 | 5.318 |
| **Maier-Kelley**** | | |
| $C_P^\circ = a + bT + cT^{-2}$ | | |
| a | $b\times10^3$ | $c\times10^{-5}$ |
| 9.044 | 12.34 | - 0.97895 |

* Heat capacity equation taken from Berman and Brown (1985).
** Heat capacity equation taken from Maier and Kelley (1932).

interlayer $H_2O$ estimated by Ransom and Helgeson (1994b) which are given in table 2 and those of bulk $H_2O$ generated from the computer program SUPCRT92 (Johnson, Oelkers, and Helgeson, 1992) from equations and parameters in Johnson and Norton (1991).

Combining eq (10) with the results of calculations described in app. A and the relation

$$G^\circ_{H_2O,P_r,T} - G^\circ_{H_2O,P_r,T_r} = H^\circ_{H_2O,P_r,T} - H^\circ_{H_2O,P_r,T_r} - TS^\circ_{H_2O,P_r,T} + T_rS^\circ_{H_2O,P_r,T_r} \tag{11}$$

leads to

$$\begin{aligned}\Delta G_r^\circ = {} & \Delta G^\circ_{r,P_r,T_r} + 59.18(T - T_r) + 4.5(G^\circ_{H_2O} - G^\circ_{H_2O,P_r,T_r}) \\ & - 1.852(P - P_r) - 4.5k_{0,H_2O(il)}\left((T - T_r) - T\ln\left(\frac{T}{T_r}\right)\right) \\ & - 9k_{1,H_2O(il)}\left(2T^{0.5} - T_r^{0.5} - \frac{T}{T_r^{0.5}}\right) + 2.25k_{2,H_2O(il)}\left(\frac{1}{T} - \frac{2}{T_r} + \frac{T}{T_r^2}\right) \\ & + k_{3,H_2O(il)}\left(\frac{0.75}{T^2} - \frac{2.25}{T_r^2} + \frac{1.5T}{T_r^3}\right)\end{aligned} \tag{12}$$

where $G^\circ_{H_2O,P_r,T}$, $H^\circ_{H_2O,P_r,T}$, and $S^\circ_{H_2O,P_r,T}$ stand for the standard molal Gibbs free energy, enthalpy, and entropy of bulk $H_2O$ at the subscripted temperatures and pressures, $G^\circ_{H_2O,P_r,T_r}$, $H^\circ_{H_2O,P_r,T_r}$, and $S^\circ_{H_2O,P_r,T_r}$ designate these properties at reference conditions, and $k_{0,H_2O(il)}$, $k_{1,H_2O(il)}$, $k_{2,H_2O(il)}$, and $k_{3,H_2O(il)}$ denote the Berman-Brown heat capacity power function coefficients (Berman and Brown, 1985) of interlayer $H_2O$.

The interlayer sites of most naturally occurring smectites are occupied by $Na^+$, $Ca^{2+}$, $Mg^{2+}$, and $K^+$; however, interlayer cations such as $NH_4^+$ $Rb^+$, $Cs^+$, $Ba^{2+}$, and $Sr^{2+}$ are commonly found in smectites in petroliferous shales and nuclear waste repository sites. Values of the standard molal Gibbs free energy of dehydration of these smectites at elevated temperatures and pressures were calculated from eq (12) using values of $\Delta G^\circ_{r,P_r,T_r}$ from table 1, values of $G^\circ_{H_2O} - G^\circ_{H_2O,P_r,T_r}$ for bulk $H_2O$ generated from the computer program SUPCRT92 (Johnson, Oelkers, and Helgeson, 1992), and the Berman-Brown heat capacity coefficients of interlayer $H_2O$ given in table 2. The standard molal Gibbs free energies computed in this manner were then combined with eq (9) to obtain equilibrium constants for smectite dehydration at temperatures from 25° to 300 °C and pressures from $P_{SAT}$ to 5 kb.[5] The results of these calculations are given in table 3. It follows from eq (12) that the standard molal Gibbs free energy of smectite dehydration is solely a function of the properties of bulk and interlayer $H_2O$ and the standard molal Gibbs free energy of reaction (1) at 1 bar and 25 °C. Hence, differences between the equilibrium constants shown in table 3 are due solely to differences in $\Delta G^\circ_{r,P_r,T_r}$.

Computed values of log K for the dehydration of Na- and Ca-smectite are plotted as functions of temperature and pressure in figures 1 and 2. The curves shown in these figures are representative of the temperature and pressure dependence of log K for the dehydration of all the monovalent (figs 1A, 2A) and divalent (figs 1B, 2B) cation exchanged smectites in table 1. It can be seen in figure 1 that log K for reaction (1) increases monotonically with temperature in a near linear fashion. In contrast, the curves in figure 2 representing log K as a function of pressure exhibit shallow minima with increasing pressure at temperatures $< 100$ °C. These minima result from the decrease in the standard molal volume of $H_2O$ with increasing pressure.

Procedures for calculating the standard molal entropy, volume, heat capacity, and enthalpy of smectite dehydration at elevated temperatures and pressures are described in app. B. Results of these calculations to 300 °C and 5 kb are presented in app. B in tables B.1, B.2, B.3, and B.5. Values of the reaction properties in these tables increase in magnitude with increasing temperature and decrease with increasing pressure. With the exception of values of the standard molal enthalpy at 25 °C and

[5] $P_{SAT}$ refers to pressures corresponding to the liquid-vapor equilibrium curve for the system $H_2O$, except at temperatures $< 100$ °C where it refers to the reference pressure of 1 bar.

TABLE 3

*Log K for reaction (1) in the text as a function of temperature and pressure for pure homoionic smectites with interlayer cations that commonly occur in sedimentary systems, petroliferous shales, and nuclear waste repository sites (see text)*

**Na–SMECTITE**

| | P (bars) | | | | | | | |
|---|---|---|---|---|---|---|---|---|
| T (°C) | $P_{SAT}$* | 100 | 500 | 1000 | 2000 | 3000 | 4000 | 5000 |
| 25 | - 0.77 | - 0.77 | - 0.80 | - 0.81 | - 0.81 | - 0.77 | - 0.70 | - 0.60 |
| 50 | - 0.39 | - 0.40 | - 0.42 | - 0.44 | - 0.46 | - 0.43 | - 0.38 | - 0.30 |
| 75 | 0.02 | 0.01 | - 0.02 | - 0.05 | - 0.07 | - 0.06 | - 0.03 | 0.03 |
| 100 | 0.45 | 0.43 | 0.40 | 0.36 | 0.32 | 0.32 | 0.34 | 0.38 |
| 125 | 0.88 | 0.87 | 0.83 | 0.78 | 0.73 | 0.71 | 0.72 | 0.75 |
| 150 | 1.32 | 1.31 | 1.26 | 1.21 | 1.14 | 1.11 | 1.10 | 1.11 |
| 175 | 1.76 | 1.75 | 1.69 | 1.63 | 1.55 | 1.50 | 1.48 | 1.48 |
| 200 | 2.20 | 2.18 | 2.12 | 2.05 | 1.95 | 1.89 | 1.86 | 1.85 |
| 225 | 2.63 | 2.62 | 2.54 | 2.47 | 2.36 | 2.28 | 2.24 | 2.22 |
| 250 | 3.07 | 3.05 | 2.97 | 2.88 | 2.75 | 2.67 | 2.61 | 2.58 |
| 275 | 3.49 | 3.48 | 3.38 | 3.29 | 3.14 | 3.04 | 2.98 | 2.94 |
| 300 | 3.92 | 3.91 | 3.80 | 3.69 | 3.52 | 3.41 | 3.33 | 3.28 |

**K–SMECTITE**

| | P (bars) | | | | | | | |
|---|---|---|---|---|---|---|---|---|
| T (°C) | $P_{SAT}$* | 100 | 500 | 1000 | 2000 | 3000 | 4000 | 5000 |
| 25 | - 0.15 | - 0.16 | - 0.18 | - 0.20 | - 0.20 | - 0.16 | - 0.08 | 0.01 |
| 50 | 0.18 | 0.17 | 0.15 | 0.12 | 0.11 | 0.14 | 0.19 | 0.27 |
| 75 | 0.55 | 0.54 | 0.51 | 0.48 | 0.45 | 0.46 | 0.50 | 0.56 |
| 100 | 0.94 | 0.93 | 0.89 | 0.86 | 0.82 | 0.81 | 0.83 | 0.88 |
| 125 | 1.34 | 1.33 | 1.29 | 1.24 | 1.19 | 1.17 | 1.18 | 1.21 |
| 150 | 1.75 | 1.74 | 1.69 | 1.64 | 1.57 | 1.54 | 1.53 | 1.55 |
| 175 | 2.17 | 2.15 | 2.10 | 2.04 | 1.96 | 1.91 | 1.89 | 1.89 |
| 200 | 2.59 | 2.57 | 2.51 | 2.44 | 2.34 | 2.28 | 2.25 | 2.24 |
| 225 | 3.00 | 2.99 | 2.91 | 2.84 | 2.72 | 2.65 | 2.61 | 2.59 |
| 250 | 3.42 | 3.40 | 3.32 | 3.23 | 3.10 | 3.02 | 2.96 | 2.93 |
| 275 | 3.83 | 3.82 | 3.72 | 3.62 | 3.48 | 3.38 | 3.31 | 3.27 |
| 300 | 4.24 | 4.23 | 4.12 | 4.01 | 3.84 | 3.73 | 3.65 | 3.60 |

**$NH_4$–SMECTITE**

| | P (bars) | | | | | | | |
|---|---|---|---|---|---|---|---|---|
| T (°C) | $P_{SAT}$* | 100 | 500 | 1000 | 2000 | 3000 | 4000 | 5000 |
| 25 | - 0.09 | - 0.10 | - 0.12 | - 0.14 | - 0.14 | - 0.10 | - 0.03 | 0.07 |
| 50 | 0.23 | 0.23 | 0.20 | 0.18 | 0.17 | 0.19 | 0.24 | 0.32 |
| 75 | 0.60 | 0.59 | 0.56 | 0.53 | 0.50 | 0.51 | 0.55 | 0.61 |
| 100 | 0.98 | 0.97 | 0.94 | 0.90 | 0.86 | 0.86 | 0.88 | 0.92 |
| 120 | 1.38 | 1.87 | 1.33 | 1.29 | 1.23 | 1.21 | 1.22 | 1.25 |
| 150 | 1.79 | 1.78 | 1.73 | 1.68 | 1.61 | 1.58 | 1.57 | 1.59 |
| 175 | 2.21 | 2.19 | 2.14 | 2.08 | 2.00 | 1.95 | 1.93 | 1.93 |
| 200 | 2.62 | 2.61 | 2.54 | 2.48 | 2.38 | 2.32 | 2.29 | 2.28 |
| 225 | 3.04 | 3.02 | 2.95 | 2.87 | 2.76 | 2.68 | 2.64 | 2.62 |
| 250 | 3.45 | 3.43 | 3.35 | 3.26 | 3.13 | 3.05 | 2.99 | 2.96 |
| 275 | 3.86 | 3.85 | 3.75 | 3.65 | 3.51 | 3.41 | 3.34 | 3.30 |
| 300 | 4.27 | 4.26 | 4.15 | 4.04 | 3.87 | 3.76 | 3.68 | 3.63 |

* See footnote 5.

TABLE 3
*(continued)*

**Rb–SMECTITE**

| T (°C) | $P_{SAT}$* | P (bars) 100 | 500 | 1000 | 2000 | 3000 | 4000 | 5000 |
|---|---|---|---|---|---|---|---|---|
| 25 | 0.04 | 0.03 | 0.01 | - 0.01 | - 0.01 | 0.03 | 0.11 | 0.20 |
| 50 | 0.36 | 0.35 | 0.32 | 0.30 | 0.29 | 0.31 | 0.37 | 0.44 |
| 75 | 0.71 | 0.70 | 0.67 | 0.64 | 0.62 | 0.63 | 0.66 | 0.72 |
| 100 | 1.09 | 0.08 | 1.04 | 1.01 | 0.97 | 0.96 | 0.98 | 1.03 |
| 125 | 1.48 | 1.47 | 1.43 | 1.39 | 1.33 | 1.31 | 1.32 | 1.35 |
| 150 | 1.89 | 1.87 | 1.82 | 1.78 | 1.71 | 1.67 | 1.67 | 1.68 |
| 175 | 2.30 | 2.28 | 2.22 | 2.17 | 2.08 | 2.04 | 2.02 | 2.02 |
| 200 | 2.71 | 2.69 | 2.63 | 2.56 | 2.46 | 2.40 | 2.37 | 2.36 |
| 225 | 3.12 | 3.10 | 3.03 | 2.95 | 2.84 | 2.76 | 2.72 | 2.70 |
| 250 | 3.53 | 3.51 | 3.43 | 3.34 | 3.21 | 3.12 | 3.07 | 3.04 |
| 275 | 3.93 | 3.92 | 3.82 | 3.72 | 3.58 | 3.48 | 3.41 | 3.37 |
| 300 | 4.33 | 4.33 | 4.22 | 4.11 | 3.94 | 3.83 | 3.75 | 3.70 |

**Cs–SMECTITE**

| T (°C) | $P_{SAT}$* | P (bars) 100 | 500 | 1000 | 2000 | 3000 | 4000 | 5000 |
|---|---|---|---|---|---|---|---|---|
| 25 | 0.28 | 0.27 | 0.25 | 0.23 | 0.23 | 0.27 | 0.34 | 0.44 |
| 50 | 0.57 | 0.57 | 0.54 | 0.52 | 0.51 | 0.53 | 0.58 | 0.66 |
| 75 | 0.91 | 0.90 | 0.87 | 0.84 | 0.82 | 0.83 | 0.86 | 0.93 |
| 100 | 1.28 | 1.27 | 1.23 | 1.20 | 1.16 | 1.15 | 1.17 | 1.22 |
| 125 | 1.66 | 1.65 | 1.61 | 1.56 | 1.51 | 1.49 | 1.50 | 1.53 |
| 150 | 2.05 | 2.04 | 1.99 | 1.94 | 1.87 | 1.84 | 1.83 | 1.85 |
| 175 | 2.45 | 2.44 | 2.38 | 2.32 | 2.24 | 2.19 | 2.17 | 2.18 |
| 200 | 2.86 | 2.84 | 2.77 | 2.71 | 2.61 | 2.55 | 2.52 | 2.51 |
| 225 | 3.26 | 3.24 | 3.17 | 3.09 | 2.98 | 2.91 | 2.86 | 2.84 |
| 250 | 3.66 | 3.65 | 3.56 | 3.47 | 3.35 | 3.26 | 3.20 | 3.17 |
| 275 | 4.06 | 4.05 | 3.95 | 3.85 | 3.71 | 3.61 | 3.54 | 3.50 |
| 300 | 4.46 | 4.45 | 4.34 | 4.23 | 4.07 | 3.95 | 3.88 | 3.83 |

**Ca–SMECTITE**

| T (°C) | $P_{SAT}$* | P (bars) 100 | 500 | 1000 | 2000 | 3000 | 4000 | 5000 |
|---|---|---|---|---|---|---|---|---|
| 25 | - 3.61 | - 3.62 | - 3.64 | - 3.66 | - 3.66 | - 3.61 | - 3.54 | - 3.45 |
| 50 | - 3.01 | - 3.02 | - 3.05 | - 3.07 | - 3.08 | - 3.05 | - 3.00 | - 2.92 |
| 75 | - 2.42 | - 2.42 | - 2.46 | - 2.48 | - 2.51 | - 2.50 | - 2.46 | - 2.40 |
| 100 | - 1.83 | - 1.84 | - 1.87 | - 1.91 | - 1.95 | - 1.95 | - 1.93 | - 1.89 |
| 125 | - 1.25 | - 1.26 | - 1.30 | - 1.35 | - 1.40 | - 1.42 | - 1.41 | - 1.38 |
| 150 | - 0.68 | - 0.70 | - 0.75 | - 0.80 | - 0.86 | - 0.90 | - 0.90 | - 0.89 |
| 175 | - 0.13 | - 0.15 | - 0.20 | - 0.26 | - 0.34 | - 0.39 | - 0.41 | - 0.41 |
| 200 | 0.41 | 0.39 | 0.33 | 0.26 | 0.16 | 0.10 | 0.07 | 0.06 |
| 225 | 0.93 | 0.92 | 0.84 | 0.77 | 0.65 | 0.58 | 0.54 | 0.52 |
| 250 | 1.45 | 1.43 | 1.35 | 1.26 | 1.13 | 1.04 | 0.99 | 0.96 |
| 275 | 1.95 | 1.93 | 1.84 | 1.74 | 1.59 | 1.50 | 1.43 | 1.39 |
| 300 | 2.44 | 2.43 | 2.32 | 2.21 | 2.04 | 1.93 | 1.86 | 1.81 |

* See footnote 5.

TABLE 3

*(continued)*

**Mg–SMECTITE**

| T (°C) | $P_{SAT}$* | P (bars) 100 | 500 | 1000 | 2000 | 3000 | 4000 | 5000 |
|---|---|---|---|---|---|---|---|---|
| 25 | - 4.28 | - 4.29 | - 4.31 | - 4.33 | - 4.33 | - 4.29 | - 4.22 | - 4.12 |
| 50 | - 3.63 | - 3.64 | - 3.66 | - 3.69 | - 3.70 | - 3.67 | - 3.62 | - 3.54 |
| 75 | - 2.99 | - 3.00 | - 3.03 | - 3.06 | - 3.08 | - 3.07 | - 3.04 | - 2.98 |
| 100 | - 2.36 | - 2.37 | - 2.41 | - 2.44 | - 2.48 | - 2.49 | - 2.47 | - 2.42 |
| 125 | - 1.75 | - 1.76 | - 1.81 | - 1.85 | - 1.90 | - 1.92 | - 1.92 | - 1.89 |
| 150 | - 1.16 | - 1.17 | - 1.22 | - 1.27 | - 1.34 | - 1.37 | - 1.38 | - 1.36 |
| 175 | - 0.58 | - 0.59 | - 0.65 | - 0.71 | - 0.79 | - 0.84 | - 0.86 | - 0.85 |
| 200 | - 0.02 | - 0.03 | - 0.10 | - 0.16 | - 0.26 | - 0.32 | - 0.35 | - 0.36 |
| 225 | 0.53 | 0.51 | 0.44 | 0.36 | 0.25 | 0.18 | 0.13 | 0.12 |
| 250 | 1.06 | 1.05 | 0.96 | 0.88 | 0.75 | 0.66 | 0.61 | 0.58 |
| 275 | 1.58 | 1.57 | 1.47 | 1.37 | 1.23 | 1.13 | 1.06 | 1.02 |
| 300 | 2.09 | 2.08 | 1.97 | 1.86 | 1.70 | 1.58 | 1.51 | 1.46 |

**Sr–SMECTITE**

| T (°C) | $P_{SAT}$* | P (bars) 100 | 500 | 1000 | 2000 | 3000 | 4000 | 5000 |
|---|---|---|---|---|---|---|---|---|
| 25 | - 3.38 | - 3.39 | - 3.42 | - 3.43 | - 3.43 | - 3.39 | - 3.32 | - 3.22 |
| 50 | - 2.80 | - 2.81 | - 2.84 | - 2.86 | - 2.87 | - 2.85 | - 2.79 | - 2.72 |
| 75 | - 0.22 | - 2.23 | - 2.26 | - 2.29 | - 2.32 | - 2.31 | - 2.27 | - 2.21 |
| 100 | - 1.65 | - 1.66 | - 1.69 | - 1.73 | - 1.77 | - 1.77 | - 1.75 | - 1.71 |
| 125 | - 1.08 | - 1.09 | - 1.14 | - 1.18 | - 1.23 | - 1.25 | - 1.24 | - 1.21 |
| 150 | - 0.53 | - 0.54 | - 0.59 | - 0.64 | - 0.71 | - 0.74 | - 0.75 | - 0.73 |
| 175 | 0.02 | 0.00 | - 0.05 | - 0.11 | - 0.19 | - 0.24 | - 0.26 | - 0.26 |
| 200 | 0.55 | 0.53 | 0.47 | 0.40 | 0.30 | 0.24 | 0.21 | 0.20 |
| 225 | 1.07 | 1.05 | 0.98 | 0.90 | 0.79 | 0.71 | 0.67 | 0.65 |
| 250 | 1.57 | 1.56 | 1.47 | 1.39 | 1.26 | 1.17 | 1.12 | 1.09 |
| 275 | 2.07 | 2.06 | 1.96 | 1.86 | 1.72 | 1.62 | 1.55 | 1.51 |
| 300 | 2.55 | 2.55 | 2.43 | 2.32 | 2.16 | 2.05 | 1.97 | 1.92 |

**Ba–SMECTITE**

| T (°C) | $P_{SAT}$* | P (bars) 100 | 500 | 1000 | 2000 | 3000 | 4000 | 5000 |
|---|---|---|---|---|---|---|---|---|
| 25 | - 3.05 | - 3.05 | - 3.08 | - 3.09 | - 3.09 | - 3.05 | - 2.98 | - 2.88 |
| 50 | - 2.49 | - 2.50 | - 2.53 | - 2.55 | - 2.56 | - 2.54 | - 2.48 | - 2.40 |
| 75 | - 1.93 | - 1.94 | - 1.97 | - 2.00 | - 2.03 | - 2.02 | - 1.98 | - 1.92 |
| 100 | - 1.38 | - 1.39 | - 1.42 | - 1.46 | - 1.50 | - 1.50 | - 1.48 | - 1.44 |
| 125 | - 0.83 | - 0.84 | - 0.88 | - 0.92 | - 0.98 | - 1.00 | - 0.99 | - 0.96 |
| 150 | - 0.29 | - 0.30 | - 0.35 | - 0.40 | - 0.47 | - 0.50 | - 0.51 | - 0.49 |
| 175 | 0.24 | 0.23 | 0.17 | 0.11 | 0.03 | - 0.02 | - 0.04 | - 0.03 |
| 200 | 0.76 | 0.75 | 0.68 | 0.61 | 0.52 | 0.46 | 0.42 | 0.42 |
| 225 | 1.27 | 1.25 | 1.18 | 1.10 | 0.99 | 0.92 | 0.87 | 0.85 |
| 250 | 1.77 | 1.75 | 1.67 | 1.58 | 1.45 | 1.37 | 1.31 | 1.28 |
| 275 | 2.25 | 2.24 | 2.14 | 2.04 | 1.90 | 1.80 | 1.73 | 1.69 |
| 300 | 2.73 | 2.72 | 2.61 | 2.50 | 2.34 | 2.23 | 2.15 | 2.10 |

* See footnote 5.

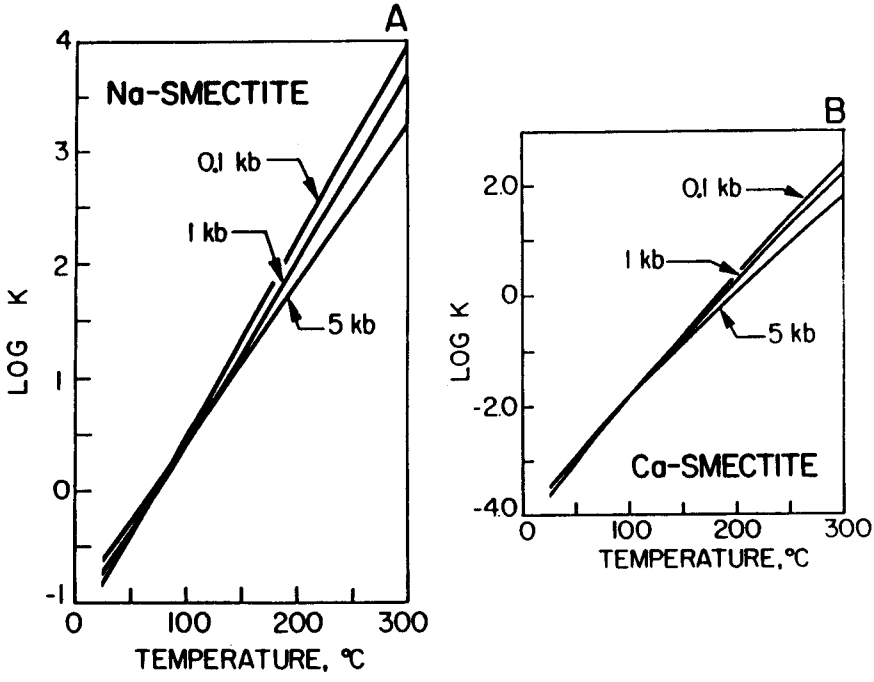


Fig. 1. Log K for the dehydration of pure Na-smectite (A) and pure Ca-smectite (B) as a function of temperature at constant pressure (labeled in kilobars)—see text.

pressures above 100 bar and those of the standard molal volume at low temperatures and pressures above 2 kb, these reaction properties are positive. It can be seen in table B.5 in app. B that the standard molal enthalpy of reaction (1) is positive along crustal geotherms. Thus the smectite dehydration reaction is endothermic. Along crustal geotherms, the volume of reaction (1) is also positive in sign because at these conditions the density of interlayer $H_2O$ is greater than that of bulk $H_2O$ (Ransom and Helgeson, 1994a). Therefore, in geologic systems the standard molal volume of hydrated smectite is less than that of its dehydrated counterpart and the volume of bulk $H_2O$ evolved in the reaction.

## SMECTITE DEHYDRATION IN SEDIMENTARY BASINS AS A FUNCTION OF DEPTH AND TEMPERATURE

In order to relate the thermodynamic calculations summarized above to geologic coordinates represented by depth and temperature, the dependence of temperature and fluid pressure on depth in sedimen-

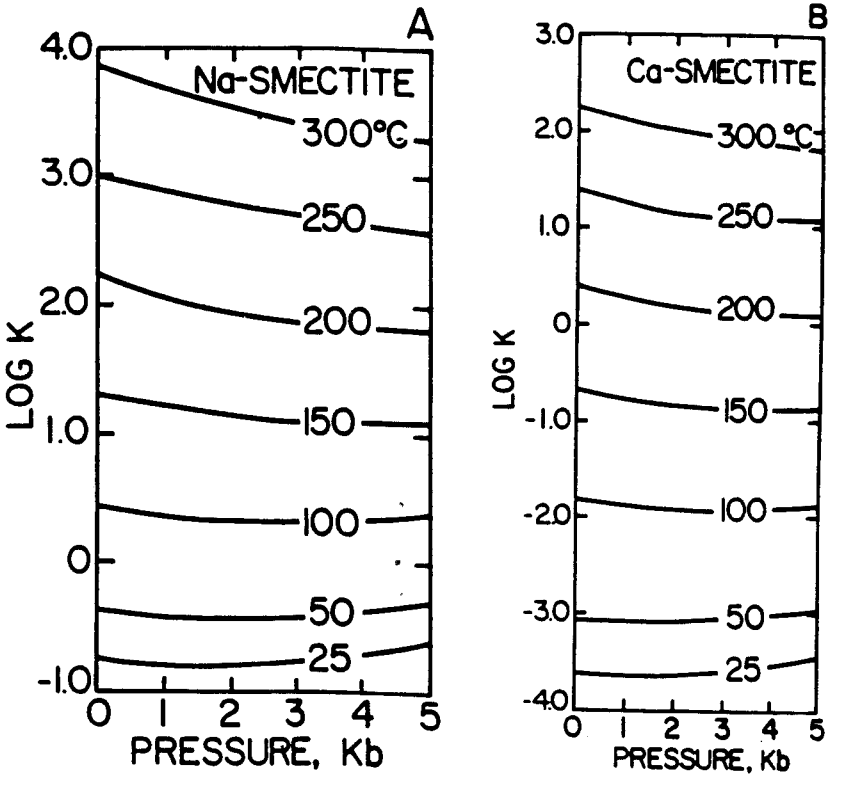


Fig. 2. Log K for the dehydration of pure Na-smectite (A) and pure Ca-smectite (B) as a function of pressure at constant temperature (labeled in °C)—see text.

tary basins must be established.[6] This has been done in many parts of the Tertiary sedimentary basin off the Mississippi-Louisiana-Texas coast of the United States (U.S. Gulf Coast). For example, Burst (1969) and Hower and others (1976) report temperature-depth profiles for these sediments. Pressure-depth gradients have been reported by Dickinson (1953), Stuart (1970), Barker (1972), Parker (1974), Magara (1975), Graf (1982), Barker and Horsfield (1982), Bethke (1986), Harrison and Summa (1991), and others. Representative data taken from Hower and others (1976), Burst (1969), and Stuart (1970) were used in the present study to generate typical pressure-temperature profiles for the U.S. Gulf Coast

[6] It has been shown that in non-hydrostatically stressed systems such as sedimentary basins, thermodynamic equilibrium between minerals and aqueous solutions at a given temperature and bulk composition depends on the fluid pressure not the overburden pressure (Bruton and Helgeson, 1983; Holdaway and Goodge, 1990).

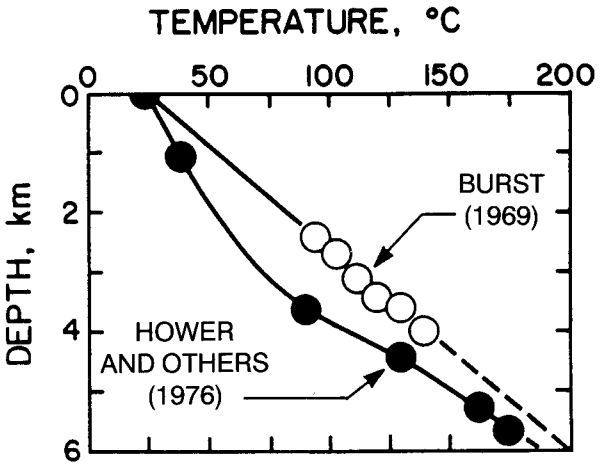


Fig. 3. Geothermal profiles reported by Hower and others (1976) (black circles) and Burst (1969) (white circles) for Tertiary US Gulf Coast sediments.

Tertiary section. These profiles are used below to illustrate the consequences of smectite dehydration during burial and diagenesis.

*Pressure-temperature-depth relations in the U.S. Gulf Coast.*—Geothermal gradients in the Gulf Coast vary from 18 °C $km^{-1}$ to ~36 °C $km^{-1}$ (Jam, Dickey, and Eysteinn, 1969). However, owing to lithologic and hydrologic discontinuities, they are not necessarily constant with depth. Temperatures reported by Burst (1969) and Hower and others (1976) are plotted in figure 3. It can be seen in this figure that the curve representing downhole temperatures reported by Burst (1969) is nearly linear with an average gradient of 26 °C $km^{-1}$. In contrast, the geotherm generated from data given by Hower and others (1976) exhibits considerable curvature. This profile has an average gradient of 18 °C $km^{-1}$ down to 3 km where it changes to 31 °C $km^{-1}$. The break in slope at ~3 km coincides with the depth at which pore fluid pressure begins to exceed the hydrostatic pressure.

Pressure-depth profiles taken from Stuart (1970) are shown in figure 4. The geostatic curve in this figure represents the pressure exerted by the overburden and includes contributions from the changing salinity and density of pore fluids with depth, the average densities of the minerals in the section, the relative proportions of sandstone and shale in the stratigraphic column, and the net porosities of the various lithologies. In contrast to the geostatic curve that changes monotonically with depth, the curve representing fluid pressure exhibits drastic changes in slope at depths near 3 km. Above 3 km, the fluid pressure curve corresponds to the hydrostatic gradient of a typical Gulf Coast subsurface brine (Dickinson, 1953; Stuart, 1970). Just below 3 km, the slope of this curve becomes abruptly less negative with increasing depth, resulting in a pressure

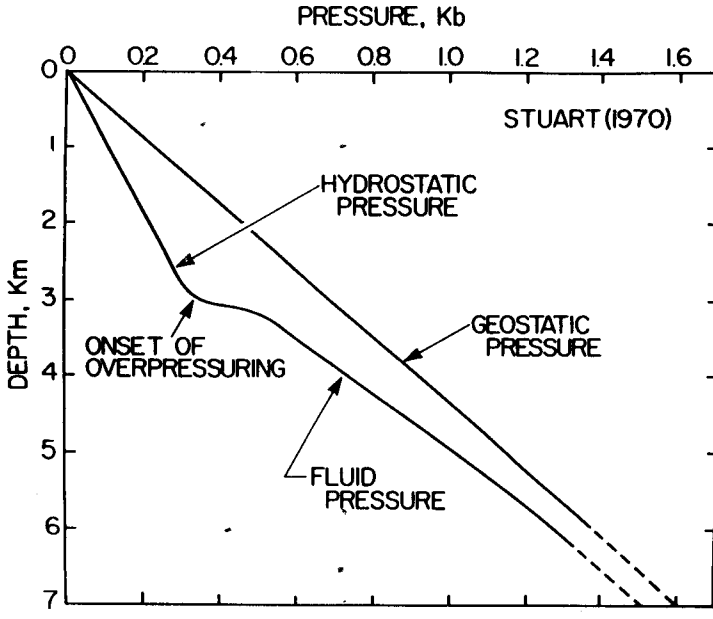


Fig. 4. Geostatic and fluid pressure profiles generated by Stuart (1970) for Tertiary sediments in the Gulf Coast of the United States. The geostatic pressure gradient is consistent with a bulk sediment density of 2.26 g $cm^{-3}$. The hydrostatic pressure segment of the fluid pressure profile corresponds to that of an NaCl brine with a salinity of 80,000 ppm. The rapid increase in fluid pressure just below 3 km marks the onset of overpressuring (see text).

increase of 200 bars over a depth interval of only 150 m. This break in slope marks the onset of overpressuring in Gulf Coast sediments.[7] At fluid pressures above 500 bars, the fluid pressure gradient changes gradually, approaching that of the average geostatic gradient by about 6 km.

Temperature-pressure profiles consistent with the curves depicted in figures 3 and 4 are shown in figure 5. In figure 5, the solid lines (A and B) represent fluid pressures along the Burst and Hower geotherms, and the dashed lines (C and D) designate corresponding geostatic pressures. The onset of overpressuring occurs at approx 75 °C for curve A and 115 °C for curve B.

*Calculation of the extent of dehydration of homoionic smectites during burial diagenesis.*—The pressure-temperature coordinates represented by curves A and B in figure 5 permit calculation of the equilibrium hydration state of smectite with increasing burial along the geothermal profiles shown in

[7] Overpressured (also known as geopressured) sedimentary sections are those for which the reported fluid pressures are greater than those generated by hydrostatic pressure at a corresponding depth.

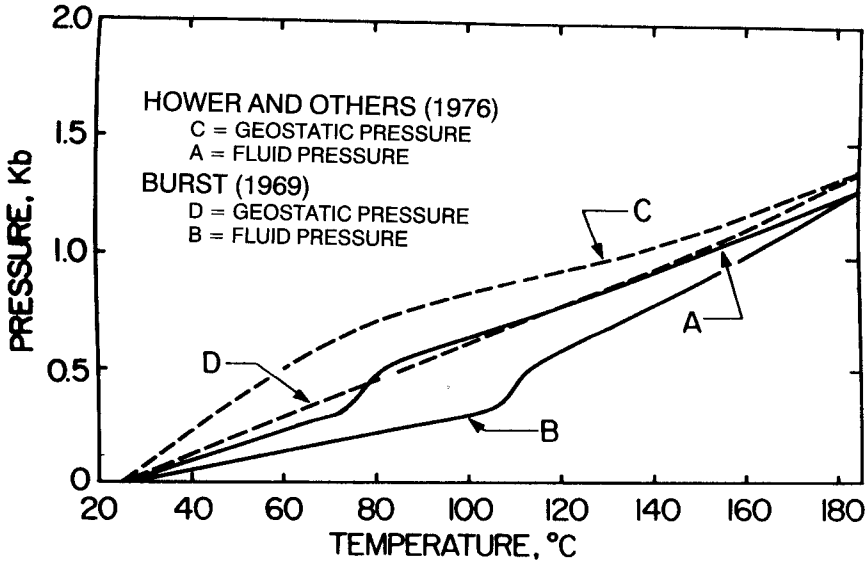


Fig. 5. Temperature-pressure curves for Tertiary Gulf Coast sediments. The curves were generated by combining the geotherms in figure 3 with the geostatic and fluid pressure profiles in figure 4.

figure 3. Homogeneous equilibrium for a solid solution of hydrous and anhydrous smectite components in equilibrium with an aqueous phase for which $a_{H_2O} \approx 1$ is represented by eq (8) for a given temperature and pressure.[8] Combining eq (8) with pressures and temperatures along curves A and B in figure 5, values of $W_s$ in table 1, and those of log K computed from eqs (9) to (12), values of $X_{hs}$ in smectite can be calculated as a function of temperature and pressure in the U.S. Gulf Coast sedimentary section. The results of such calculations for Na-, Ca- and K-smectite are shown in figures 6 to 8. It can be seen in these figures that pure Na- and K-smectite at equilibrium are only partially hydrated at pressures and temperatures corresponding to those on or near the Earth's surface. In contrast, similar calculations indicate that Ca-smectite is almost completely hydrated under these conditions. Note that $X_{hs}$ for Na- and K-smectite decreases from 0.62 and 0.52, respectively, at 25 °C to almost 0.1 at 200 °C. Hence, at low temperatures, the monovalent cation-exchanged smectites are about 40 to 50 percent dehydrated. This dehydration increases to more than 90 percent at temperatures near 250 °C. In contrast, values of $X_{hs}$ for Ca-smectite range from about 1.0 at

[8] It has been documented that the activity of $H_2O$ in electrolyte solutions such as formation waters and oil field brines decreases by less than ~0.1 with increasing molality of NaCl and/or other electrolytes to ~3 molal at the temperatures and pressures shown in figures 6 to 8 (Helgeson, Kirkham, and Flowers, 1981; Pitzer, Peiper, and Busey, 1984).

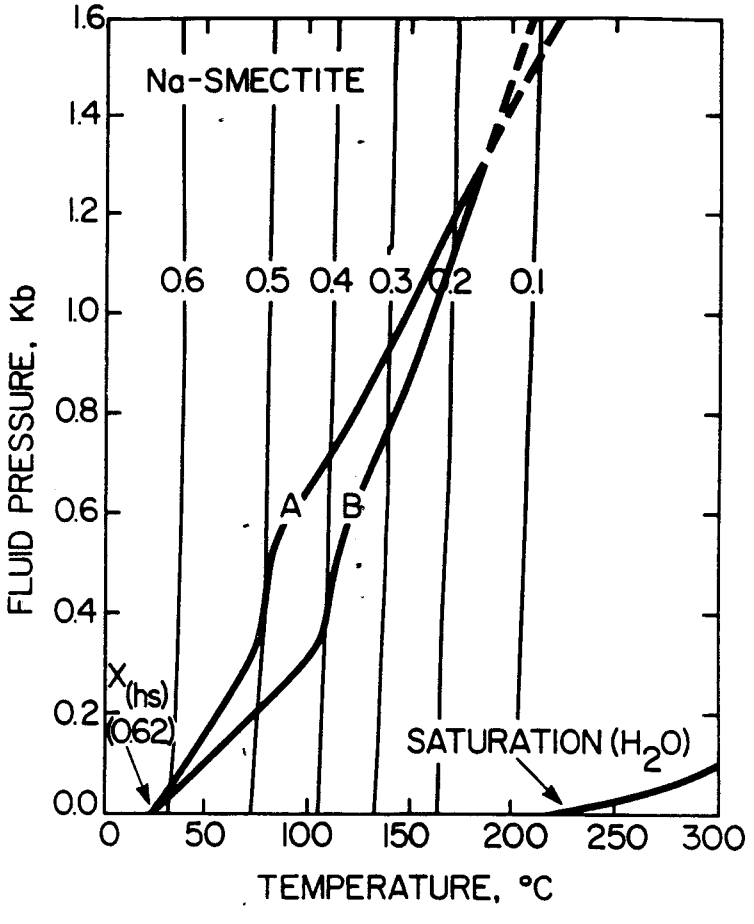


Fig. 6. Isopleths representing the mole fraction of the hydrous smectite component of Na-smectite ($X_{hs}$) as a function of temperature and fluid pressure. Curves A and B correspond to those with the same labels in figure 5, and the curve marked SATURATION ($H_2O$) represents the liquid-vapor equilibrium curve for $H_2O$ (see footnote 5).

25 °C to 0.4 at 200 °C (fig 7). Equilibrium calculations thus indicate that pure Ca-smectite is substantially more hydrated at all temperatures and pressures than either Na- or K-smectite. Note that isopleths of $X_{hs}$ in figures 6 to 8 are nearly parallel to the segments of curves A and B which represent the onset of overpressuring in the Gulf Coast. It thus appears that the abrupt increase in fluid pressure observed in Gulf Coast sediments at ~3 km is not a result of smectite dehydration.

Because $Ca^{+2}$, $Na^+$, and $K^+$ commonly dominate the interlayer sites of smectites found in sedimentary basins, the isopleths of $X_{hs}$ in figures 7

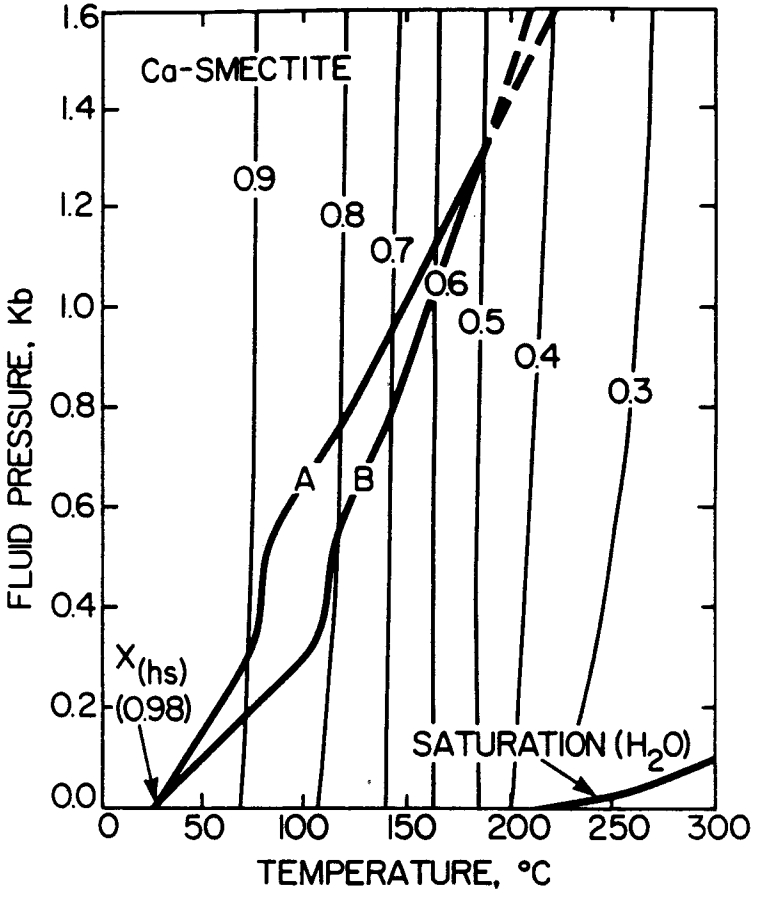


Fig. 7. Isopleths representing the mole fraction of the hydrous smectite component of Ca-smectite ($X_{hs}$) as a function of temperature and fluid pressure (see caption of fig. 6).

and 8 represent approximate maximum and minimum equilibrium hydration states, respectively, of smectites in argillaceous sediments. The extent to which interlayers in smectites in nature are hydrated beyond that shown in figures 6 and 8 can be attributed to solid solution with Ca-, Mg- or other divalent cation-exchanged smectite components.[9]

[9] The hydration states calculated in the present study indicate only the amount of interlayer $H_2O$ present in the mineral. This is not necessarily the same as the water content of a clay, as the water content includes contributions from pore and surface adsorbed $H_2O$. These latter contributions depend strongly on the surface area of the crystallites in the sample (Ransom and Helgeson, 1994a).

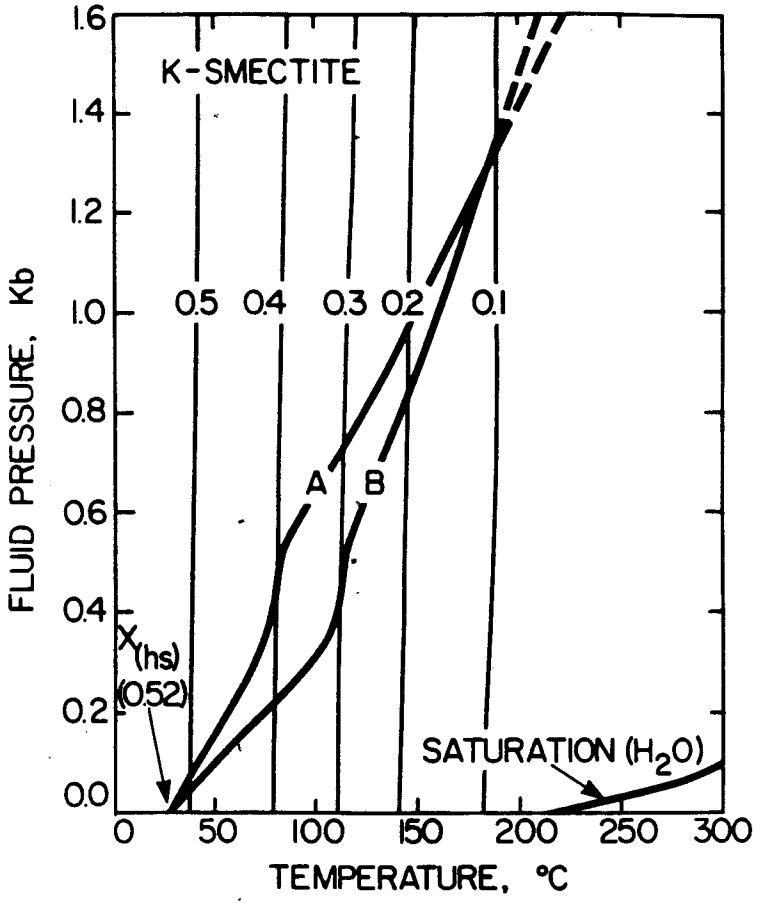


Fig. 8. Isopleths representing the mole fraction of the hydrous smectite component of K-smectite ($X_{hs}$) as a function of temperature and fluid pressure (see captionof fig. 6).

## PREDICTED DEGREES OF SMECTITE DEHYDRATION IN ARGILLACEOUS SEDIMENTS DURING BURIAL AND DIAGENESIS

It can be deduced from figures 6 to 8 that the extent to which smectite dehydrates with increasing depth depends not only on temperature and pressure but also on the identities of the interlayer cations in the mineral. Bulk chemical analyses demonstrate that smectites in nature contain more than one type of interlayer cation. The most common interlayer cations are $Na^+$, $Ca^{2+}$, and $K^+$. Therefore, it seems likely that the hydration state of smectite at any particular pressure and temperature depends on the extent to which Na-, K-, and/or Ca-smectite compo-

nents are present in the solid solution. Taking account of the close similarities in the degree of hydration of Na- and K-smectite at various temperatures and pressures (figs. 6 and 8), the combined dehydration of the Na- and K-components of smectite solid solutions is described below solely in terms of the Na-smectite component. Hence, for the purpose of the following calculations, the interlayer composition of smectite in natural systems was taken to be thermodynamically consistent with a binary solid solution of Na- and Ca-smectite components.

Homogeneous equilibrium in a (Ca, Na)-smectite solid solution can be described in terms of the law of mass action for dehydration reactions involving the hydrous and anhydrous thermodynamic components of the endmembers of the binary solution. The components chosen to express these reactions correspond to those generated from smectite compositions reported in the literature (Ransom and Helgeson, 1993). Accordingly, the dehydration of (Na, Ca)-smectite can be expressed by writing

$$\underset{\text{(hydrous smectite component)}}{NaAl_3Si_3O_{10}(OH)_2 \cdot 4.5\ H_2O} \rightleftarrows \underset{\text{(anhydrous smectite component)}}{NaAl_3Si_3O_{10}(OH)_2} + 4.5\ H_2O \qquad (13)$$

and

$$\underset{\text{(hydrous smectite component)}}{Ca_{0.5}Al_3Si_3O_{10}(OH)_2 \cdot 4.5\ H_2O} \rightleftarrows \underset{\text{(anhydrous smectite component)}}{Ca_{0.5}Al_3Si_3O_{10}(OH)_2} + 4.5\ H_2O. \qquad (14)$$

The law of mass action for reactions 13 and 14 can be expressed for $a_{H_2O} \approx 1$ as

$$\log K_{13} = \log\left(\frac{a_{Na(as)}}{a_{Na(hs)}}\right) \equiv \log\left(\frac{X_{Na(as)}}{X_{Na(hs)}}\right) + \log\left(\frac{\lambda_{Na(as)}}{\lambda_{Na(hs)}}\right) \qquad (15)$$

and

$$\log K_{14} = \log\left(\frac{a_{Ca(as)}}{a_{Ca(hs)}}\right) \equiv \log\left(\frac{X_{Ca(as)}}{X_{Ca(hs)}}\right) + \log\left(\frac{\lambda_{Ca(as)}}{\lambda_{Ca(hs)}}\right) \qquad (16)$$

where $K_{13}$ and $K_{14}$ stand for the equilibrium constants of the subscripted reactions, and $X_{Na(hs)}$, $X_{Na(as)}$, $X_{Ca(hs)}$, $X_{Ca(as)}$, and $\lambda_{Na(hs)}$, $\lambda_{Na(as)}$, $\lambda_{Ca(hs)}$, and $\lambda_{Ca(as)}$ refer to the mole fractions and activity coefficients, respectively, of the subscripted hydrous and anhydrous Na- and Ca- components of the solid solution. Assuming that the Na- and Ca-smectite components mix ideally (Tardy and Fritz, 1981), it follows that the regular solution Margules parameters given in table 1 for solid solutions of homologous hydrous and anhydrous Na- and Ca-smectite components ($W_{Na}$ and $W_{Ca}$, respectively) are independent of the mole fractions of these components. Hence, the activity coefficients of the Na- and Ca- components of the binary solid solution can be expressed in terms of their Margules parameters and mole fractions of the hydrous and anhydrous components.

Accordingly, eqs (15) and (16) can be written as

$$\log K_{13} = \log\left(\frac{X_{Na(as)}}{X_{Na(hs)}}\right) + \frac{W_{Na}}{2.303\ RT}\left[(1 - X_{Na(as)})^2 - (1 - X_{Na(hs)})^2\right] \quad (17)$$

and

$$\log K_{14} = \log\left(\frac{X_{Ca(as)}}{X_{Ca(hs)}}\right) + \frac{W_{Ca}}{2.303\ RT}\left[(1 - X_{Ca(as)})^2 - (1 - X_{Ca(hs)})^2\right] \quad (18)$$

Taking account of the conservation of mass represented by

$$X_{Na} + X_{Ca} = 1, \quad (19)$$

we can write

$$X_{Na} = X_{Na(hs)} + X_{Na(as)} \quad (20)$$

and

$$X_{Ca} = X_{Ca(hs)} + X_{Ca(as)} \quad (21)$$

where $X_{Na}$ and $X_{Ca}$ denote the total mole fraction of the Na- and Ca-smectite components of the solid solution, respectively. Similarly, the total mole fraction of the hydrous and anhydrous components ($X_h$ and $X_a$, respectively) in the solid solution can be expressed as

$$X_h = X_{Na(hs)} + X_{Ca(hs)} \quad (22)$$

and

$$X_a = X_{Na(as)} + X_{Ca(as)} \quad (23)$$

which is consistent with

$$X_h + X_a = 1 \quad (24)$$

Combining eqs (22) to (24) with eq (18) leads to

$$\log K_{14} = \log\left(\frac{X_a - X_{Na(as)}}{1 - X_a - X_{Na(hs)}}\right) + \frac{W_{Ca}}{2.303\ RT}\left[(1 - X_a - X_{Na(as)})^2 - (X_a - X_{Na(hs)})^2\right]. \quad (25)$$

Simultaneously solving eqs (17) and (25) using values of $W_s$ taken from table 1 and those of log K computed from eqs (9) and (12) permits calculation of $X_{Na(hs)}$, $X_{Na(as)}$, $X_{Ca(hs)}$, and $X_{Ca(as)}$ as a function of $X_a$ with depth in the U.S. Gulf Coast. Conversely, $X_a$ can be computed from compositional data from which the mole fractions of the various smectite layer components (for example, $X_{Na}$ or $X_{Ca}$) have been determined.

## DISCUSSION

Reliable compositional data for smectite interlayer cation compositions that are required to solve eqs (17) to (25) for $X_a$ are scarce because bulk chemical analyses of clay samples, most of which contain a heterogeneous mix of minerals, do not permit unequivocal assignment of elements to mineral stoichiometries when more than one mineral in the sample contains the same element (for example, potassium is found in illite, smectite, k-feldspar, et cetera). Requisite compositional information can be obtained, however, from analytical transmission electron microscope (ATEM) analyses of smectites (Ahn and Peacor, 1986). Unfortunately, at present there are insufficient compositional data of this kind to document such profiles. Nevertheless, estimated smectite compositions can be used to predict likely hydration states for smectite solid solutions as a function of depth in sedimentary basins.

If, as suggested by Ransom and Helgeson (1994a), the hydrous and anhydrous thermodynamic components of regular smectite solid solutions have physical significance, natural undisturbed smectites should exhibit random mixed-layering of expanded (hydrous) and collapsed (anhydrous) layers.[10] According to the calculations presented above, the number of collapsed layers in such smectites should progressively increase with burial depth. To illustrate the application of eqs (1) to (25) to thermodynamic analysis of smectite dehydration in sedimentary basins, a hypothetical depth profile representing a likely distribution of hydrated and collapsed smectite layers for a binary solid solution of Na- and Ca-smectite components is shown in figure 9. In this example, hydrated smectite layers make up the bulk of the sediment at depths less than 3 km with collapsed layers increasing progressively with depth. The shaded area from 3.0 to 3.25 km in the figure represents the onset of overpressuring in the U.S. Gulf Coast.

Simultaneously solving eqs (17) and (25) using values of $W_s$ in table 1, together with those of $X_a$ consistent with the curve in figure 9 and values of log K computed from eqs (9) and (12), permits evaluation of eqs (19) to (21). The results of these calculations are depicted in figures 10 to 13. It can be deduced from these figures that at shallow burial depths where smectite expandabilities (that is, numbers of hydrated layers) are large, $Ca^{2+}$ predominates in the interlayer. However, with increasing depth, smectite becomes progressively enriched in the Na component of the solid solution. By ~3.5 km, monovalent cations occupy virtually all the interlayer sites in the mineral. This compositional trend is consistent with

[10] It should be noted that this mixed-layering does not arise from physical mixing or the intergrowth of smectite with illite or other 10Å micas, but is instead a consequence of the solid solubility of smectite components that differ in composition by the presence or absence of interlayer $H_2O$. In accord with Ransom and Helgeson (1989), the term illite is used in the present communication to refer to the mineral, not to nonexpandable layers of uncertain composition exhibiting 10 Å basal spacings. Similarly, the term smectite is used to designate the mineral, not layers that simply expand upon exposure to water, ethylene glycol, or other solvents.

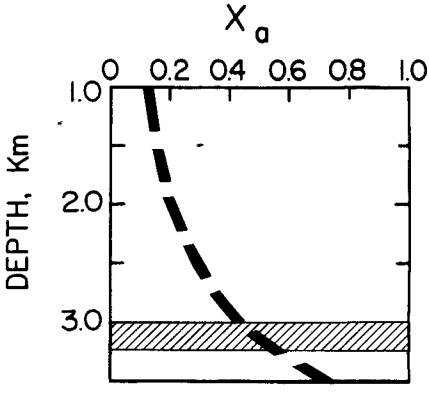


Fig. 9. Hypothetical depth profile representing a likely distribution of the mole fraction of anhydrous (collapsed) smectite layers ($X_a$) in U.S. Gulf Coast sediments. The dark band at 3 to 3.25 km represents depths corresponding to the onset of overpressuring (see fig. 4).

analytical transmission electron microscope studies (Ahn and Peacor, 1986) which show that in the U.S. Gulf Coast, smectite at depth contains only interlayer Na and K, with no evidence of Ca and Mg which dominate the interlayer sites of smectites deposited at the Gulf of Mexico sediment-water interface.

Values of $X_{Na(hs)}$ and $X_{Ca(hs)}$ computed from the curve in figure 9 and the equations given above are shown in figures 11 and 12, respectively, as a function of $X_h$. It can be seen in figure 11 that the calculated mole fraction of the hydrous Na-smectite component of the (Na, Ca)-smectite solid solution increases from about 0.13 at 1 km to 0.37 at 3 km. In contrast, the mole fraction of the hydrous Ca-smectite component decreases from 0.75 at 1 km to 0.25 at 3 km as $X_h$ in the smectite solid solution decreases with depth (fig. 12). The number of moles of interlayer $H_2O$ retained at equilibrium by the binary smectite solid solution under consideration is plotted as a function of depth in figure 13. It can be deduced from this figure that the increase in $X_{Na}$ at the expense of $X_{Ca}$ with increasing depth results at 3.5 km in a smectite with 60 to 65 percent less interlayer $H_2O$ per mole than that present at the Earth's surface (that is, ~4.5 moles of interlayer $H_2O$ per mole of smectite). This observation has far-reaching implications with respect to diagenesis and the amount of intracrystalline interlayer $H_2O$ that can be released to pore spaces by the reaction of smectite to form illite and other authigenic minerals at depth in sedimentary basins.

The example above describes the consequences of homogeneous equilibrium. However, conditions in natural systems may prevent equilibrium from being obtained. In this regard it should be noted that the change in the standard molal volume of the dehydration reaction is positive along crustal geotherms (table B.2 in app. B). If this volume

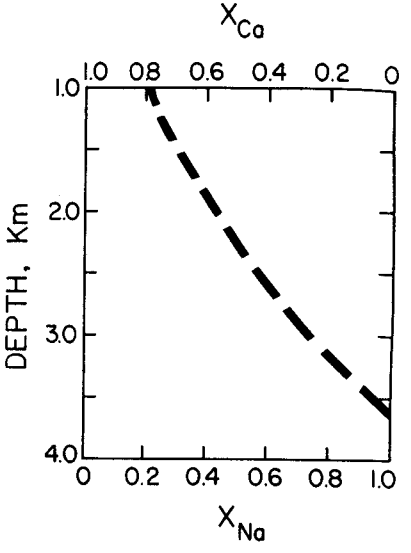


Fig. 10. Calculated mole fractions of the Na- and Ca-smectite components of the binary smectite solid solution represented by the depth profile in figure 9 (see text).

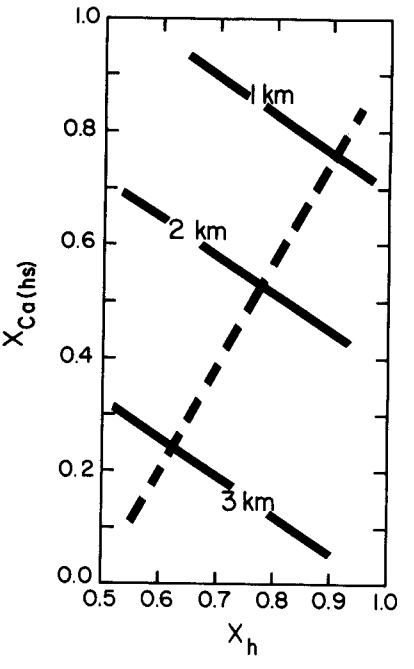


Fig. 12. Calculated mole fraction of the hydrous Ca-smectite component ($X_{Ca(hs)}$) as a function of the mole fraction of the hydrous component ($X_h$) of the smectite solid solution represented by the profile in figure 9 (see text). Contours indicate increasing depth from 1 to 3 km.

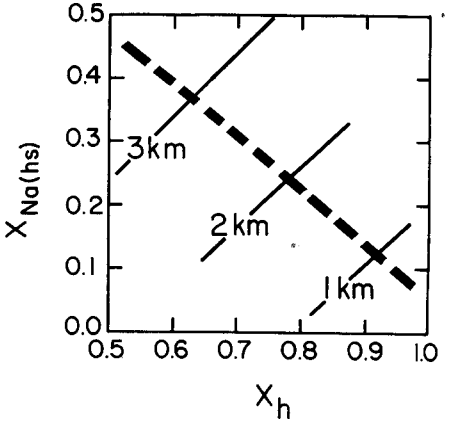


Fig. 11. Calculated mole fraction of the hydrous Na-smectite component ($X_{Na(hs)}$) as a function of the mole fraction of the hydrous component ($X_h$) of the smectite solid solution represented by the curve in figure 9 (see text). Contours indicate increasing depth from 1 to 3 km.

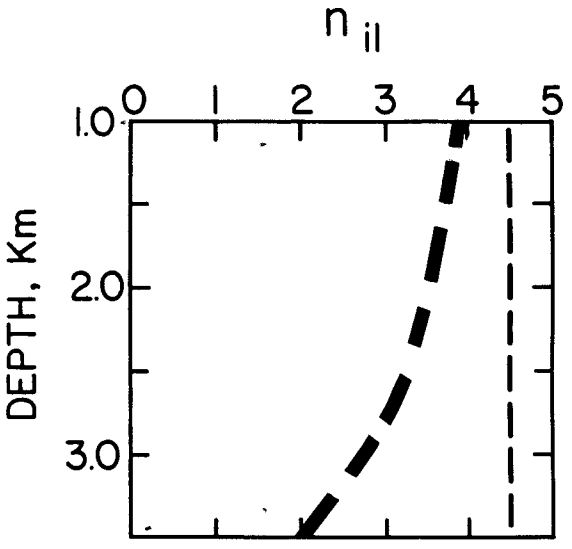


Fig. 13. Depth profile representing the number of moles of interlayer $H_2O$ per mole of smectite in the solid solution represented by the curve in figure 9. The vertical line designates the number of moles of interlayer $H_2O$ in one mole of the smectite solid solution at Earth surface conditions ($\sim 4.5$).

change is supressed due to burial or tectonic forces, then the hydration state of smectite would not be that of the equilibrium value but would be held metastably at higher values of $X_h$. This provides a mechanism for episodic fluid generation that would coincide with sudden pressure releases such as failures along faults. Dehydration of smectite in this case would take place rapidly. A consequence of such dehydration episodes would be the depression of the local geothermal gradient as the dehydration reaction is endothermic at crustal conditions (table B.5).

## CONCLUDING REMARKS

The thermodynamic calculations carried out in the present study indicate that interlayer dehydration is an inevitable consequence of smectite burial in sedimentary basins. The relations summarized above make it possible to assess the equilibrium hydration state of smectite at temperatures and depths along crustal geotherms, as well as volume and enthalpy changes that occur during the reaction. Results of such calculations suggest that the amount of interlayer $H_2O$ retained in smectite at depth in the U.S. Gulf Coast may be far less than is generally thought to be the case. It appears likely that in the U.S. Gulf Coast, the equilibrium interlayer hydration state of smectite at 3 to 3.5 km is only about 60 to 65 percent of that at the surface. This diminished hydration state decreases considerably the amount of fluid that can be produced by reactions in which smectite reacts to form authigenic minerals such as illite or chlorite. In contrast, the calculations indicate that interlayer dehydration of

smectite at shallower depths may lead to the expulsion of more pore water in the upper hydrostatically-dominated part of the section than previously thought. Because the standard molal volume of smectite dehydration is positive, a sudden pressure release such as failure along a local fault could trigger smectite dehydration, resulting in an episode of rapid fluid generation accompanied by a short term depression of the local geothermal gradient.

The observations and conclusions summarized in the preceding pages suggest several avenues of research that need innovative experimental investigation and that are necessary to confirm the results of this study. Primary among these is a comparison of the chemistry, structure, hydration state, and thermodynamic behavior of smectite in natural systems with those of samples prepared for laboratory study (Ahn and Peacor, 1986; Vali, Hesse, and Martin, 1994). To do so requires the development and refinement of nondestructive sample preparation techniques that preserve in an unaltered state the chemistry, hydration state, and structural integrity of smectite crystallites. In addition, new and novel analytical methods are needed to examine the textural, physical, and chemical characteristics of these crystallites. Only then will it be possible to understand fully the behavior of smectite in geologic processes.

ACKNOWLEDGMENTS

The present communication represents part of the senior author's Ph.D. dissertation at the University of California at Berkeley. The research was supported by the National Science Foundation (NSF grants EAR 77-14492, EAR 81-15859, EAR 8606052, and EAR-9117393), the Department of Energy (DOE contract DE-AT03-83ER-13100 and grant DE-FG03-85ER-13419), and the Committee on Research at the University of California. Part of the research was carried out in Professor Volkmar Trommsdorf's laboratory at the ETH in Zurich, Switzerland and in Professor Yves Tardy's laboratory at the University Louis Pasteur in Strasbourg, France. The warm hospitality and many stimulating interchanges we enjoyed in these laboratories are acknowledged with thanks. We are indebted to Eric Oelkers, Edward Warren, Paul Nadeau, Denny Eberl, Vitalii Pokrovskii, Jan Amend, Everett Shock, Bill Murphy, and Peter Lichtner for helpful discussions and suggestions during the course of this study.

## APPENDIX A

## *Derivation and calculation of* $\Delta S^\circ_{r,P_r,T_r}$, $\int_{P_r}^{P} \Delta V^\circ_r \, dP$, *and* $\Delta C^\circ_{P_r,r}$ *for smectite dehydration in sedimentary basins*

*The standard molal entropy and volume of smectite dehydration in eq (10) in the text.* The standard molal entropy and volume of reaction (1) in the text at 1 bar and 25 °C can be calculated only if the corresponding properties of bulk and interlayer $H_2O$ and those of the anhydrous and hydrous components of the smectite solid solution are known. Values of the standard molal entropy and volume of bulk $H_2O$ were computed from the equation of state given by Johnson and Norton (1991). Values of interlayer $H_2O$ were taken from Ransom and Helgeson (1994b). Values of the standard molal entropies and volumes of many of the

anhydrous components of smectite solid solutions (for example, $NaAl_3Si_3O_{10}(OH)_2$, $KAl_3Si_3O_{10}(OH)_2$, et cetera, Ransom and Helgeson, 1993), can be taken directly from calorimetric or volume data available in the literature, from compilations of thermodynamic data (Helgeson and others, 1978; Robie, Hemingway, and Fisher, 1978; Holland, 1988), or calculated from appropriate additivity and structural analog algorithms (Ransom and Helgeson 1994b). Direct measurement of the standard molal entropy and volume of the hydrous smectite components used in this study are not possible because they have fictive compositions. Nevertheless, values of $\Delta S^\circ_{r,P_r,T_r}$ and $\int_{P_r}^{P} \Delta V^\circ_r dP$ in eq. (10) in the text can be estimated using a difference algorithm for the hypothetical *intracrystalline* reaction represented by

$$\text{hs} \rightleftarrows \text{as} + 4.5\ H_2O(il) \tag{A.1}$$

where hs and as stand for the hydrous and anhydrous thermodynamic components of smectite, $H_2O(il)$ refers to interlayer $H_2O$, and 4.5 represents the numbers of moles of interlayer $H_2O$ in one mole of the hydrous smectite component (Ransom and Helgeson, 1994a).

Numerous algorithms have been proposed to estimate the standard molal entropies and volumes of minerals at 25 °C and 1 bar (Fyfe, Turner, and Verhoogen, 1958; Robinson and Haas, 1976; Helgeson and others, 1978; Holland, 1988; Ransom and Helgeson, 1994b). These generally provide close approximations and are based on corresponding states relations, additivity rules, and/or the entropies or volumes of structural analogs of the minerals for which properties are to be estimated. For example, taking account of intracrystalline reaction (A.1), the differences between the standard molal entropies and volumes of homologous hydrous and anhydrous smectite components at 1 bar and 25 °C ($\delta S^\circ_{s,P_r,T_r}$ and $\delta V^\circ_{s,P_r,T_r}$, respectively) can be computed from

$$\delta S^\circ_{s,P_r,T_r} \equiv S^\circ_{hs,P_r,T_r} - S^\circ_{as,P_r,T_r} = 4.5\ S^\circ_{H_2O(il),P_r,T_r} - \Delta S^\circ_{r(A.1),P_r,T_r} \tag{A.2}$$

and

$$\delta V^\circ_{s,P_r,T_r} \equiv V^\circ_{hs,P_r,T_r} - V^\circ_{as,P_r,T_r} = 4.5\ V^\circ_{H_2O(il),P_r,T_r} - \Delta V^\circ_{r(A.1),P_r,T_r} \tag{A.3}$$

where $S^\circ_{H_2O(il),P_r,T_r}$ and $V^\circ_{H_2O(il),P_r,T_r}$ represent the standard molal entropy and volume of interlayer $H_2O$, respectively, $\Delta S^\circ_{r(A.1),P_r,T_r}$ and $\Delta V^\circ_{r(A.1),P_r,T_r}$ refer to the standard molal entropy and volume of reaction (A.1), and $S^\circ_{hs,P_r,T_r}$, $S^\circ_{as,P_r,T_r}$, $V^\circ_{hs,P_r,T_r}$ and $V^\circ_{as,P_r,T_r}$ designate the standard molal entropies and volumes of the subscripted homologous hydrous and anhydrous smectite components (see Ransom and Helgeson, 1994a, 1994b). Following Helgeson and others (1978), the standard molal entropies and volumes of intracrystalline reaction (A.1) can be regarded as zero. Accordingly, the values of the standard molal entropy and volume of interlayer $H_2O$ in table 2 were combined with eqs (A.2) and (A.3) to compute $\delta S^\circ_{s,P_r,T_r}$ and $\delta V^\circ_{s,P_r,T_r}$. These calculations yield 59.18 cal $mol^{-1}$ $K^{-1}$ and 77.5 $cm^3$ $mol^{-1}$, respectively. Therefore, $\Delta S^\circ_{r,P_r,T_r}$ and $\Delta V^\circ_{r,P_r,T_r}$ can be expressed for reaction (1) in the text as

$$\Delta S^\circ_{r,P_r,T_r} = 4.5\ S^\circ_{H_2O,P_r,T_r} - \delta S^\circ_{s,P_r,T_r} = 4.5\ S^\circ_{H_2O,P_r,T_r} - 59.18 \text{ cal mol}^{-1}\ \text{K}^{-1} \tag{A.4}$$

and

$$\Delta V^\circ_{r,P_r,T_r} = 4.5\ V^\circ_{H_2O,P_r,T_r} - \delta V^\circ_{s,P_r,T_r} = 4.5\ V^\circ_{H_2O,P_r,T_r} - 77.5 \text{ cm}^3 \text{ mol}^{-1} \tag{A.5}$$

where $S^\circ_{H_2O,P_r,T_r}$ and $V^\circ_{H_2O,P_r,T_r}$ denote the standard molal entropy and volume of bulk $H_2O$, respectively, at 25 °C and 1 bar. Because the standard molal entropy and volume of reaction (A.1) are taken to be zero (see above), it follows that values of $\Delta S^\circ_{r,P_r,T_r}$ and $\Delta V^\circ_{r,P_r,T_r}$ computed from eqs (A.4) and (A.5) apply equally to all smectite dehydration reactions, regardless of the compositions of the homologous hydrous and anhydrous components making up the solid solution.

Increases in both temperature and pressure have opposing effects and modify only slightly the standard molal volumes of minerals at pressures and temperatures in the Earth's crust (Helgeson and others, 1978). Accordingly, we can write for the pressures and temperatures encountered in sedimentary basins

$$\delta V_s^\circ \approx \delta V_{s,P_r,T_r}^\circ \tag{A.6}$$

where $\delta V_s^\circ$ represents the difference between the standard molal volumes of the hydrous and anhydrous components of smectite solid solutions at the pressure and temperature of interest, eq (A.5) can thus be written as

$$\Delta V_r^\circ = 4.5\ V_{H_2O}^\circ - \delta V_s^\circ = 4.5\ V_{H_2O}^\circ - 77.5\ cm^3\ mol^{-1} \tag{A.7}$$

where $V_{H_2O}^\circ$ represents the standard molal volume of bulk $H_2O$ at the temperature and pressure of interest. Using eq (A.7), the pressure integral in eq (10) in the text can be expressed as

$$\int_{P_r}^{P} \Delta V_r^\circ\, dP = 4.5\ (G_{H_2O}^\circ - G_{H_2O,P_r,T}^\circ) - 77.5\ (0.0239)\ (P - P_r) \tag{A.8}$$

where $G_{H_2O}^\circ$ and $G_{H_2O,P_r,T}^\circ$ stand for the standard molal Gibbs free energy of bulk $H_2O$ at the pressure and temperature of interest and at the subscripted pressure and temperature, respectively, and 0.0239 represents the factor for converting $cm^3\ mol^{-1}$ to cal $mol^{-1}$ $bar^{-1}$.

*The standard molal heat capacity of smectite dehydration in eq (10) in the text.*—The standard molal heat capacity of a mineral at 1 bar can be closely estimated from corresponding values of $C_{P_r}^\circ$ for the crystalline oxides and a mineral in the same structural class by assuming that the standard molal heat capacity of reaction between the two minerals and the oxides in the reaction is zero (Helgeson and others, 1978). Accordingly, $\Delta C_{P_r,r}^\circ$ in eq (10) in the text was computed in a manner analogous to that used above to estimate the standard molal entropy and volume of intracrystalline smectite dehydration.

The heat capacity analog of eq (A.3) for the difference ($\delta C_{P_r,s}^\circ$) between the standard molal heat capacities of homologous hydrous ($C_{P_r,hs}^\circ$) and anhydrous ($C_{P_r,as}^\circ$) smectite components at 1 bar and any temperature is given by

$$\delta C_{P_r,s}^\circ \equiv C_{P_r,hs}^\circ - C_{P_r,as}^\circ = 4.5\ C_{P_r,H_2O(il)}^\circ - \Delta C_{P_r,r(A.1)}^\circ \tag{A.9}$$

where $C_{P_r,H_2O(il)}^\circ$ and $\Delta C_{P_r,r(A.1)}^\circ$ refer to the standard molal heat capacity of interlayer $H_2O$ and intracrystalline reaction (A.1), respectively, at 1 bar and the temperature of interest. Combining the Berman-Brown heat capacity power function (Berman and Brown, 1985) for interlayer $H_2O$ as a function of temperature at 1 bar with eq (A.9) and assuming $\Delta C_{P_r,r(A.1)}^\circ = 0$ (see above) leads to

$$\delta C_{P_r,s}^\circ = 4.5 \left( k_{0,H_2O(il)} + \frac{k_{1,H_2O(il)}}{T^{0.5}} + \frac{k_{2,H_2O(il)}}{T^2} + \frac{k_{3,H_2O(il)}}{T^3} \right) \tag{A.10}$$

where $k_{0,H_2O(il)}$, $k_{1,H_2O(il)}$, $k_{2,H_2O(il)}$, $k_{3,H_2O(il)}$ stand for the Berman-Brown heat capacity power function coefficients for interlayer $H_2O$. Accordingly, $\Delta C_{P_r,r}^\circ$ in eq (10) in the text can be expressed for reaction (1) in the text as

$$\Delta C_{P_r,r}^\circ = 4.5\ C_{P_r,H_2O}^\circ - \delta C_{P_r,s}^\circ. \tag{A.11}$$

Combining eqs (A.10) and (A.11) leads to

$$\Delta C_{P_r,r}^\circ = 4.5\ C_{P_r,H_2O}^\circ - 4.5 \left( k_{0,H_2O(il)} + \frac{k_{1,H_2O(il)}}{T^{0.5}} + \frac{k_{2,H_2O(il)}}{T^2} + \frac{k_{3,H_2O(il)}}{T^3} \right) \tag{A.12}$$

where $C^\circ_{P_r,H_2O}$ designates the standard molal heat capacity of bulk $H_2O$ at 1 bar and the temperature of interest. Eq (A.12), together with the equation of state for bulk $H_2O$ given by Johnson and Norton (1991) and with the values of the Berman-Brown heat capacity power function coefficients for interlayer $H_2O$ listed in table 2, permits evaluation of $\Delta C^\circ_{P_r,r}$ in eq (10) in the text. In the case of the entropies and volumes estimated above, heat capacities computed from eq (A.12) apply equally to all smectite dehydration reactions.

## Appendix B

## *Derivation and calculation of $\Delta S^\circ_r$, $\Delta V^\circ_r$, $\Delta C^\circ_{P,r}$, and $\Delta H^\circ_r$ for smectite dehydration at elevated temperatures and pressures*

The calculations summarized below were carried out with the aid of the computer program SUPCRT92 (Johnson, Oelkers, and Helgeson, 1992). This program can be used to generate the electrostatic and standard molal thermodynamic properties of bulk $H_2O$ from equations given by Johnson and Norton (1991).

*Standard molal entropy of smectite dehydration.*—The standard molal entropy of reaction (1) in the text as a function of temperature and pressure ($\Delta S^\circ_r$) can be expressed as

$$\Delta S^\circ_r = \Delta S^\circ_{r,P_r,T_r} - \int_{P_r}^{P} \left( \left( \frac{\partial \Delta V^\circ_r}{\partial T} \right)_P \right)_T dP + \int_{T_r}^{T} \Delta C^\circ_{P,r} \, d \ln T \qquad (B.1)$$

where $\Delta S^\circ_{r,P_r,T_r}$ stands for the standard molal entropy of the dehydration reaction at the reference temperature and pressure, $\Delta C^{\circ *}_{P,r}$ refers to the standard molal heat capacity of dehydration at 1 bar, and $\Delta V^\circ_r$ designates the standard molal volume of reaction at the temperature and pressure of interest. Combining eq (A.12) and the partial derivative of eq (A.7) with respect to temperature at constant pressure from app. A, together with eq (B.1) leads to

$$\Delta S^\circ_r = \Delta S^\circ_{r,P_r,T_r} - 4.5 \int_{P_r}^{P} \left( \left( \frac{\partial \Delta V^\circ_{H_2O}}{\partial T} \right)_P \right)_T dP + 4.5 \int_{T_r}^{T} \Delta C^\circ_{P,H_2O} \, d \ln T$$
$$-4.5 \int_{T_r}^{T} \left( k_{0,H_2O(il)} + \frac{k_{1,H_2O(il)}}{T^{0.5}} + \frac{k_{2,H_2O(il)}}{T^2} + \frac{k_{3,H_2O(il)}}{T^3} \right) d \ln T \qquad (B.2)$$

where $V^\circ_{H_2O}$ denotes the standard molal volume of bulk $H_2O$, $C^\circ_{P_r,H_2O}$ represents the standard molal heat capacity of bulk $H_2O$ at 1 bar, and $k_{0,H_2O(il)}$, $k_{1,H_2O(il)}$, $k_{2,H_2O(il)}$, and $k_{3,H_2O(il)}$ denote the standard molal heat capacity power function coefficients of interlayer $H_2O$. Expressing $\Delta S^\circ_{r,P_r,T_r}$ in terms of eq (A.4) in app. A, eq (B.2) can be written as

$$\Delta S^\circ_r = 4.5 \, S^\circ_{H_2O,P_r,T} - 4.5 \int_{P_r}^{P} \left( \left( \frac{\partial V^\circ_{H_2O}}{\partial T} \right)_P \right)_T dP - 4.5 \, k_{0,H_2O(il)} \left( \ln \frac{T}{T_r} \right)$$
$$+ 9 \, k_{1,H_2O(il)} \left( \frac{1}{T^{0.5}} - \frac{1}{T_r^{0.5}} \right) + 2.25 \, k_{2,H_2O(il)} \left( \frac{1}{T^2} - \frac{1}{T_r^2} \right)$$
$$+ 1.5 \, k_{3,H_2O(il)} \left( \frac{1}{T^3} - \frac{1}{T_r^3} \right) - 59.18 \text{ cal mol}^{-1} \text{ K}^{-1} \qquad (B.3)$$

where $S^\circ_{H_2O,P_r,T}$ refers to the standard molal entropy of bulk $H_2O$ at the subscripted pressure and temperature. Values of $\Delta S^\circ_r$ for reaction (1) in the text were calculated from eq (B.3) for temperatures from 25° to 300° C and pressures from $P_{SAT}$ (see footnote 5) to 5 kb using the Berman-Brown heat capacity power function coefficients in table 2. The results of the calculations are shown in table B.1. Because the standard molal entropy of intracrystalline reaction (A.1) in app. A is taken to be zero, the entropies of dehydration in table B.1 are the same for all smectite solid solutions.

*Standard molal volume of smectite dehydration.*—The standard molal volume of reaction (1) in the text as a function of pressure and temperature ($\Delta V_r^\circ$) was computed from eq (A.7) in app. A. The results of these calculations for temperatures from 25° to 300° C and pressures from $P_{SAT}$ to 5 kb are given in table B.2 Like the entropies in table B.1, the standard molal volumes in table B.2 depend solely on the thermodynamic properties of bulk and interlayer $H_2O$. Hence, the standard molal volumes of reaction are the same for all binary smectite solid solutions such as those listed in table 1.

*Standard molal heat capacity of smectite dehydration.*—The standard molal heat capacity of reaction (1) in the text as a function of temperature and pressure ($\Delta C^\circ_{P_r,r}$) can be expressed as

$$\Delta C^\circ_{P,r} = \Delta C^\circ_{P_r,r} - T\int_{P_r}^{P}\left(\left(\frac{\partial^2 \Delta V_r^\circ}{\partial T^2}\right)_P\right)_T dP. \qquad (B.4)$$

Combining eq (A.12) and the second partial derivative with respect to temperature at constant pressure of eq (A.7) from app. A, together with eq (B.4) leads to

$$\Delta C^\circ_{P,r} = 4.5\, C^\circ_{P_r,H_2O} - 4.5\left(k_{0,H_2O(il)} + \frac{k_{1,H_2O(il)}}{T^{0.5}} + \frac{k_{2,H_2O(il)}}{T^2} + \frac{k_{3,H_2O(il)}}{T^3}\right) - 4.5\, T\int_{P_r}^{P}\left(\left(\frac{\partial^2 V^\circ_{H_2O}}{\partial T^2}\right)_P\right)_T dP. \qquad (B.5)$$

Values of $\Delta C^\circ_{P_r,r}$ were computed from eq (B.5) using the Berman-Brown heat capacity coefficients given in table 2. The results of these calculations are shown in table B.3.

*The standard molal enthalpy of smectite dehydration.*—The standard molal enthalpy of reaction (1) in the text as a function of pressure and temperature ($\Delta H_r^\circ$) is given by

$$\Delta H_r^\circ = \Delta H^\circ_{r,P_r,T_r} + \int_{T_r}^{T}\Delta C^\circ_{P_r,r}\, dT + \int_{P_r}^{P}\left(\Delta V_r^\circ - T\left(\frac{\partial \Delta V_r^\circ}{\partial T}\right)_P\right)_T dP \qquad (B.6)$$

where $\Delta H^\circ_{r,P_r,T_r}$ denotes the standard molal enthalpy of reaction at the reference pressure and temperature. Combining eq (A.12) and the partial derivative with respect to temperature at constant pressure of eq (A.7) from app. A, together with eq (B.6) leads to

$$\Delta H_r^\circ - \Delta H^\circ_{r,P_r,T_r} = 4.5\,(H^\circ_{H_2O,P_r,T} - H^\circ_{H_2O,P_r,T_r}) - 4.5\, k_{0,H_2O(il)}\,(T - T_r) - 9\, k_{1,H_2O(il)}\,(T^{0.5} - T_r^{0.5}) + 4.5\, k_{2,H_2O(il)}\left(\frac{1}{T} - \frac{1}{T_r}\right) + 2.25\, k_{3,H_2O(il)}\left(\frac{1}{T^2} - \frac{1}{T_r^2}\right) + 4.5\int_{P_r}^{P}\left(V^\circ_{H_2O} - T\left(\frac{\partial \Delta V^\circ_{H_2O}}{\partial T}\right)_P\right)_T dP + 77.5\,(0.0239)\,(P - P_r) \qquad (B.7)$$

where $H^\circ_{H_2O,P_r,T}$ and $H^\circ_{H_2O,P_r,T_r}$ denote the standard molal enthalpy of bulk $H_2O$ at the subscripted temperatures and pressures. In accord with the approach used in app. A to compute the standard molal entropy, $\Delta H^\circ_{r,P_r,T_r}$ in eq (B.7) can be expressed as

$$\Delta H^\circ_{r,P_r,T_r} = 4.5\,\Delta H^\circ_{f,H_2O,P_r,T_r} - \delta H^\circ_{f,s,P_r,T_r} \qquad (B.8)$$

where

$$\delta H^\circ_{f,s,P_r,T_r} \equiv \Delta H^\circ_{f,hs,P_rT_r} - \Delta H^\circ_{f,as,P_r,T_r} = 4.5\,\Delta H^\circ_{f,H_2O(il),P_r,T_r} - \Delta H^\circ_{r(A.1),P_r,T_r}, \qquad (B.9)$$

$\Delta H^\circ_{f,H_2O,P_r,T_r}$ and $\Delta H^\circ_{f,H_2O(il),P_r,T_r}$ denote the standard molal enthalpy of formation of bulk and interlayer $H_2O$, respectively, from the elements at the reference pressure and temperature, $\Delta H^\circ_{r(A.1),P_r,T_r}$ designates the standard molal enthalpy at $P_r$ and $T_r$ of reaction (A.1) in app. A, and $\delta H^\circ_{f,s,P_r,T_r}$ represents the difference at 1 bar and 25°C between the standard molal enthalpy of formation from the elements of the homologous hydrous and anhydrous

smectite components ($\Delta H^\circ_{f,hs,P_r,T_r}$ and $\Delta H^\circ_{f,as,P_r,T_r}$, respectively). As for the other properties of intracrystalline reaction (A.1) in app. A, $\Delta H^\circ_{r(A.1),P_r,T_r}$ is taken to be zero. The difference function in eq (B.9) can also be expressed as

$$\delta H^\circ_{f,s,P_r,T_r} = \delta G^\circ_{f,s,P_r,T_r} + T\delta S^\circ_{f,s,P_r,T_r} \tag{B.10}$$

where $\delta G^\circ_{f,s,P_r,T_r}$ and $\delta S^\circ_{f,s,P_r,T_r}$ are defined by

$$\delta G^\circ_{f,s,P_r,T_r} \equiv \Delta G^\circ_{f,hs,P_r,T_r} - \Delta G^\circ_{f,as,P_r,T_r} \tag{B.11}$$

and

$$\delta S^\circ_{f,s,P_r,T_r} \equiv \Delta S^\circ_{f,hs,P_r,T_r} - \Delta S^\circ_{f,as,P_r,T_r}, \tag{B.12}$$

and $\Delta G^\circ_{f,hs,P_r,T_r}$, $\Delta G^\circ_{f,as,P_r,T_r}$, $\Delta S^\circ_{f,hs,P_r,T_r}$, and $\Delta S^\circ_{f,as,P_r,T_r}$ refer to the standard molal Gibbs free energy and entropy of formation from the elements of homologous hydrous and anhydrous smectite components, respectively, at 1 bar and 25 °C. Combining eq (B.11) with the standard molal Gibbs free energy of intracrystalline reaction (1) in the text, which can be expressed as

$$\Delta G^\circ_{r,P_r,T_r} = \Delta G^\circ_{f,as,P_r,T_r} + 4.5\ \Delta G^\circ_{f,H_2O,P_r,T_r} - \Delta G^\circ_{f,hs,P_r,T_r}, \tag{B.13}$$

leads to

$$\delta G^\circ_{f,s,P_r,T_r} = 4.5\ \Delta G^\circ_{f,H_2O,P_r,T_r} - \Delta G^\circ_{r,P_r,T_r}. \tag{B.14}$$

The results of these calculations can be combined with the values of $\Delta G^\circ_{r,P_r,T_r}$ in table 1 and the value of $\Delta G^\circ_{f,H_2O,P_r,T_r}$ given by Johnson and Norton (1991) to generate values of $\delta G^\circ_{f,s,P_r,T_r}$ for a variety of smectite solid solutions. The results of these calculations are given in table B.4.

By analogy with eq (A.2) in app. A, values of $\delta S^\circ_{f,s,P_r,T_r}$ in eq (B.12) can be expressed as

$$\delta S^\circ_{f,s,P_r,T_r} = 4.5\ S^\circ_{H_2O(il),P_r,T_r} - 4.5\ (S^\circ_{H_2,P_r,T_r} + 0.5\ S^\circ_{O_2,P_r,T_r}) - \Delta S^\circ_{r(A.1),P_r,T_r} \tag{B.15}$$

where $\Delta S^\circ_{r(A.1),P_r,T_r}$ denotes the change in the standard molal entropy of reaction (A.1) in app. A which is taken to be zero (see app. A), $S^\circ_{H_2O(il),P_r,T_r}$ designates the standard molal energy of interlayer $H_2O$, and $S^\circ_{H_2,P_r,T_r}$ and $S^\circ_{O_2,P_r,T_r}$ represent the standard molal entropy of hydrogen and oxygen gas, all at reference conditions. Combining eq (B.15) with the value of $S^\circ_{H_2O(il),P_r,T_r}$ in table 2 and values of $S^\circ_{H_2,P_r,T_r}$ and $S^\circ_{O_2,P_r,T_r}$ from Cox, Wagman, and Medvedev (1989) leads to $\delta S^\circ_{f,s,P_r,T_r} = -191.5$ cal mol$^{-1}$ K$^{-1}$. Substituting this value into eq (B.10), together with values of $\delta G^\circ_{f,s,P_r,T_r}$ from table B.4 permits calculation of $\delta H^\circ_{f,s,P_r,T_r}$ for the dehydration of Na-, K-, $NH_4$-, Rb-, Cs- Ca-, Mg-, Sr-, and Ba-smectite. These values are given in table B.4. The values of $\delta H^\circ_{f,s,P_r,T_r}$ shown in this table were used together with eq (B.8) and the value of the standard molal enthalpy of formation of bulk $H_2O$ from the elements at $P_r$ and $T_r$ (Johnson and Norton, 1991) to calculate values of $\Delta H^\circ_{r,P_r,T_r}$ for the smectite solid solutions. Results of these calculations are shown in table B.4.

The properties of bulk $H_2O$ were used in conjunction with the Berman-Brown heat capacity coefficients in table 2 to compute values of $\Delta H^\circ_r - \delta H^\circ_{r,P_r,T_r}$ from eq (B.7). The results of these calculations are given in table B.5 for temperatures from 25° to 300°C and pressures from $P_{SAT}$ to 5kb. Because $\Delta H^\circ_r - \Delta H^\circ_{r,P_r,T_r}$ is independent of the layer composition of smectite, the values in table B.5 apply to all binary smectite solid solutions. Values of $\Delta H^\circ_r$ for the dehydration of these smectites at elevated temperatures and pressures can be computed by combining values of $\Delta H^\circ_r - \Delta H^\circ_{r,P_r,T_r}$ in table B.5 with those of $\Delta H^\circ_{r,P_r,T_r}$ in table B.4.

TABLE B.1

*Calculated values of the standard molal entropy of reaction (1) in the text in cal $mol^{-1}$ $K^{-1}$ as a function of temperature and pressure for binary solid solutions of homologous smectite components*

| | $\Delta S_r^\circ$ | | | | | | | |
|---|---|---|---|---|---|---|---|---|
| | | P (bars) | | | | | | |
| T (°C) | $P_{SAT}$* | 100 | 500 | 1000 | 2000 | 3000 | 4000 | 5000 |
| 25 | 16.0 | 15.97 | 15.75 | 15.44 | 14.75 | 14.05 | 13.40 | 12.77 |
| 50 | 21.6 | 21.51 | 21.16 | 20.72 | 19.88 | 19.06 | 18.28 | 17.53 |
| 75 | 26.7 | 26.60 | 26.14 | 25.60 | 24.60 | 23.69 | 22.84 | 22.05 |
| 100 | 31.5 | 31.33 | 30.77 | 30.13 | 28.99 | 27.97 | 27.05 | 26.21 |
| 125 | 36.0 | 35.78 | 35.11 | 34.37 | 33.08 | 31.97 | 30.98 | 30.09 |
| 150 | 40.2 | 39.97 | 39.20 | 38.35 | 36.92 | 35.72 | 34.66 | 33.71 |
| 175 | 44.2 | 43.97 | 43.07 | 42.11 | 40.53 | 39.23 | 38.11 | 37.11 |
| 200 | 48.1 | 47.82 | 46.76 | 45.67 | 43.93 | 42.53 | 41.34 | 40.30 |
| 225 | 51.8 | 51.56 | 50.31 | 49.07 | 47.14 | 45.64 | 44.38 | 43.29 |
| 250 | 55.5 | 55.26 | 53.75 | 52.33 | 50.20 | 48.58 | 47.25 | 46.11 |
| 275 | 59.2 | 59.00 | 57.12 | 55.47 | 53.12 | 51.38 | 49.97 | 48.78 |
| 300 | 63.1 | 62.93 | 60.47 | 58.53 | 55.92 | 54.04 | 52.55 | 51.30 |

* See footnote 5.

TABLE B.2

*Calculated values of the standard molal volume of reaction (1) in the text in $cm^3$ $mol^{-1}$ as a function of temperature and pressure for binary solid solutions of homologous smectite components (see text)*

| | $\Delta V_r^\circ$ | | | | | | | |
|---|---|---|---|---|---|---|---|---|
| | | P (bars) | | | | | | |
| T (°C) | $P_{SAT}$* | 100 | 500 | 1000 | 2000 | 3000 | 4000 | 5000 |
| 25 | 4.4 | 4.04 | 2.69 | 1.20 | - 1.27 | - 3.23 | - 4.86 | - 6.28 |
| 50 | 5.1 | 4.79 | 3.46 | 2.00 | - 0.46 | - 2.45 | - 4.11 | - 5.54 |
| 75 | 6.2 | 5.88 | 4.50 | 2.99 | 0.47 | - 1.57 | - 3.28 | - 4.74 |
| 100 | 7.7 | 7.27 | 5.79 | 4.18 | 1.53 | - 0.61 | - 2.40 | - 3.93 |
| 125 | 9.4 | 8.97 | 7.32 | 5.56 | 2.71 | 0.44 | - 1.45 | - 3.06 |
| 150 | 11.5 | 10.98 | 9.09 | 7.12 | 4.01 | 1.57 | - 0.43 | - 2.14 |
| 175 | 13.9 | 13.35 | 11.12 | 8.88 | 5.43 | 2.79 | 0.64 | - 1.18 |
| 200 | 16.8 | 16.16 | 13.47 | 10.85 | 6.98 | 4.08 | 1.77 | - 0.17 |
| 225 | 20.3 | 19.53 | 16.17 | 13.07 | 8.66 | 5.47 | 2.95 | 0.87 |
| 250 | 24.5 | 23.68 | 19.31 | 15.56 | 10.48 | 6.94 | 4.20 | 1.96 |
| 275 | 29.9 | 29.01 | 23.02 | 18.37 | 12.47 | 8.51 | 5.51 | 3.09 |
| 300 | 36.9 | 36.38 | 27.47 | 21.57 | 14.63 | 10.18 | 6.89 | 4.27 |

* See footnote 5.

TABLE B.3

*Calculated values of the standard molal heat capacity of reaction (1) in the text in cal mol$^{-1}$ as a function of temperature and pressure for binary solid solutions of homologous smectite components (see text)*

| | $\Delta C^{\circ}_{P,r}$ | | | | | | | |
|---|---|---|---|---|---|---|---|---|
| | | P (bars) | | | | | | |
| T (°C) | $P_{SAT}$* | 100 | 500 | 1000 | 2000 | 3000 | 4000 | 5000 |
| 25 | 69.4 | 68.90 | 67.11 | 65.51 | 63.49 | 61.71 | 59.26 | 55.44 |
| 50 | 68.9 | 68.50 | 67.01 | 65.56 | 63.60 | 62.27 | 61.29 | 60.81 |
| 75 | 68.7 | 68.25 | 66.80 | 65.36 | 63.32 | 61.94 | 60.94 | 60.31 |
| 100 | 68.8 | 68.33 | 66.82 | 65.32 | 63.18 | 61.74 | 60.68 | 59.84 |
| 125 | 69.2 | 68.67 | 66.99 | 65.36 | 63.08 | 61.58 | 60.51 | 59.69 |
| 150 | 69.8 | 69.25 | 67.26 | 65.42 | 62.92 | 61.32 | 60.22 | 59.41 |
| 175 | 70.9 | 70.18 | 67.71 | 65.54 | 62.73 | 60.97 | 59.79 | 58.96 |
| 200 | 72.5 | 71.63 | 68.42 | 65.78 | 62.55 | 60.60 | 59.31 | 58.41 |
| 225 | 75.1 | 73.91 | 69.53 | 66.23 | 62.44 | 60.25 | 58.83 | 57.85 |
| 250 | 79.0 | 77.48 | 71.16 | 66.94 | 62.45 | 59.98 | 58.39 | 57.31 |
| 275 | 85.1 | 83.32 | 73.47 | 67.94 | 62.59 | 59.79 | 58.03 | 56.84 |
| 300 | 95.5 | 94.15 | 76.70 | 69.27 | 62.85 | 59.69 | 57.75 | 56.44 |

* See footnote 5.

TABLE B.4

*Calculated values of $\Delta H^{\circ}_{r,P_r,T_r}$, $\delta H^{\circ}_{f,s,P_r,T_r}$, and $\delta G^{\circ}_{f,s,P_r,T_r}$ in kcal mol$^{-1}$ for the dehydration of smectite at 25 °C and 1 bar expressed in terms of reaction (1) in the text*

| Solid Solution | $\delta G^{\circ}_{f,s,P_r,T_r}$ | $\delta H^{\circ}_{f,s,P_r,T_r}$ | $\Delta H^{\circ}_{r,P_r,T_r}$ |
|---|---|---|---|
| Na–smectite | - 256.139 | - 313.240 | 5.81 |
| K–smectite | - 255.299 | - 312.400 | 4.974 |
| $NH_4$–smectite | - 255.221 | - 312.322 | 4.896 |
| Rb–smectite | - 255.040 | - 312.140 | 4.714 |
| Cs–smectite | - 254.718 | - 311.818 | 4.392 |
| Mg–smectite | - 260.934 | - 318.035 | 10.609 |
| Ca–smectite | - 260.018 | - 317.119 | 9.639 |
| Sr–smectite | - 259.717 | - 316.813 | 9.387 |
| Ba–smectite | - 259.252 | - 316.352 | 8.962 |

TABLE B.5

*Calculated values of* $\Delta H^\circ_r - \Delta H^\circ_{r,P_r,T_r}$ *for reaction (1) in the text in kcal mol*$^{-1}$ *as a function of temperature and pressure for binary solid solutions of homologous smectite components*

| | $\Delta H^\circ_r - \Delta H^\circ_{r,P_r,T_r}$ | | | | | | | |
|---|---|---|---|---|---|---|---|---|
| | | P (bars) | | | | | | |
| T (°C) | $P_{SAT}$* | 100 | 500 | 1000 | 2000 | 3000 | 4000 | 5000 |
| 25 | 0 | - 0.006 | - 0.040 | - 0.110 | - 0.317 | - 0.580 | - 0.873 | - 1.192 |
| 50 | 1.729 | 1.712 | 1.638 | 1.530 | 1.274 | 0.974 | 0.644 | 0.285 |
| 75 | 3.448 | 3.421 | 3.310 | 3.167 | 2.860 | 2.527 | 2.172 | 1.801 |
| 100 | 5.165 | 5.127 | 4.980 | 4.800 | 4.441 | 4.072 | 3.692 | 3.302 |
| 125 | 6.888 | 6.840 | 6.652 | 6.433 | 6.019 | 5.614 | 5.207 | 4.796 |
| 150 | 8.623 | 8.563 | 8.330 | 8.068 | 7.591 | 7.150 | 6.717 | 6.285 |
| 175 | 10.378 | 10.305 | 10.017 | 9.705 | 9.165 | 8.679 | 8.217 | 7.765 |
| 200 | 12.163 | 12.076 | 11.817 | 11.346 | 10.731 | 10.199 | 9.706 | 9.233 |
| 225 | 13.994 | 13.893 | 13.441 | 12.995 | 12.293 | 11.709 | 11.183 | 10.686 |
| 250 | 15.892 | 15.782 | 15.198 | 14.660 | 13.854 | 13.212 | 12.648 | 12.125 |
| 275 | 17.892 | 17.786 | 17.004 | 16.345 | 15.417 | 14.709 | 14.103 | 13.552 |
| 300 | 20.047 | 19.988 | 18.879 | 18.059 | 16.984 | 16.202 | 15.550 | 14.968 |

* See footnote 5.

## REFERENCES


Ahn, J. H., and Peacor, D. R., 1986, Transmission and analytical electron microscopy of the smectite-to-illite transition: Clays and Clay Minerals, v. 34, p. 165–179.

Barker, Colin, 1972, Aquathermal pressuring—Role of temperature in development of abnormal-pressure zones: American Association of Petroleum Geologists Bulletin, v. 56, p. 2068–2071.

Barker, Colin, and Horsfield, B., 1982, Mechanical versus thermal cause of abnormally high pore pressures in shales: Discussion: American Association of Petroleum Geologists Bulletin, v. 66, p. 99–100.

Berman, R. G., and Brown, T. H., 1985, Heat capacity of minerals in the system $Na_2O$-$K_2O$-CaO-MgO-FeO-$Fe_2O_3$-$Al_2O_3$-$SiO_2$-$TiO_2$-$H_2O$-$CO_2$ representation, estimation, and high temperature extrapolation: Contributions to Mineralogy and Petrology, v. 89, p. 168–183.

Bethke, C. M., 1986, Inverse hydrologic analysis of the distribution and origin of Gulf Coast-type geopressured zones: Journal of Geophysical Research, v. 91, p. 6535–6545.

Bird, Peter, 1984, Hydration-phase diagrams and friction of montmorillonite under laboratory and geologic conditions with implications for shale compaction, slope instability, and strength of fault gouge: Tectonophysics, v. 107, p. 235–260.

Bruce, C. H., 1984, Smectite dehydration - Its relation to structural development and hydrocarbon accumulation in northern Gulf of Mexico basin: American Association of Petroleum Geologists Bulletin, v. 68, p. 673–683.

Bruton, C. J. and Helgeson, H. C., 1983, Calculation of the chemical and thermodynamic consequences of differences between fluid and geostatic pressure in hydrothermal systems: American Journal of Science, v. 283A, p. 540–588.

Burst, J. F., 1969, Diagenesis of Gulf Coast clayey sediments and its possible relation to petroleum migration: American Association of Petroleum Geologists Bulletin, v. 53, p. 73–93.

Chapman, R. E., 1972, Clays with abnormal interstitial fluid pressures: American Association of Petroleum Geologists Bulletin, v. 56, p. 790–802.
Colten, V. A., 1986, Hydration states of smectite in NaCl brines at elevated pressures and temperatures: Clays & Clay Minerals, v. 34,p. 385–389.
Colten-Bradley, V. A., 1987, Role of pressure in smectite dehydration - Effects on geopressure and smectite-to-illite transition: American Association of Petroleum Geologists Bulletin, v. 71, p. 1414–1427.
Cox, J. D., Wagman, D. D., and Medvedev, V. A., 1989, CODATA Key Values for Thermodynamics: New York, Hemisphere Publishing Corporation, 271 p.
Dickinson, George, 1953, Geological aspects of abnormal reservoir pressure in Gulf Coast Louisiana: American Association of Petroleum Geologists Bulletin, v. 37, p. 410–432.
Freed, R. L., and Peacor, D. R., 1989, Geopressured shale and sealing effect of smectite to illite transition: American Association of Petroleum Geologists Bulletin, v. 73, p. 1223–1232.
Fyfe, W. S., Turner, F. J., and Verhoogen, J. Fyfe, 1958, Metamorphic reactions and metamorphic facies: Geological Society of America Memoir, v. 75, p. 1–253.
Graf, D. L., 1982, Chemical osmosis, reverse chemical osmosis, and the origin of subsurface brines: Geochimica et Cosmochimica Acta, v. 46, p. 1431–1448.
Hall, P. L., Astill, D. M., and McConnell, J. D. C., 1986, Thermodynamic and structural aspects of the dehydration of smectites in sedimentary rocks: Clay Minerals, v. 21, p. 633–648.
Harrison, W. J., and Summa, L. L., 1991, Paleohydrology of the Gulf of Mexico basin: American Journal of Science, v. 291, p. 109–176.
Helgeson, H. C., Delany, J. M., Nesbitt, W. H., and Bird, D. K., 1978, Summary and critique of the thermodynamic properties of rock-forming minerals: American Journal of Science, v. 278-A, p. 1–229.
Helgeson, H. C., Kirkham, D. H., and Flowers, G. C., 1981, Theoretical prediction of the thermodynamic behavior of aqueous electrolytes at high pressures and temperatures: IV. Calculation of activity coefficients, osmotic coefficients, and apparent molal and standard and relative partial molal properties to 600°C and 5kb: American Journal of Science, v. 281, p. 1249–1516.
Holdaway, M. J., and Goodge, J. W., 1990, Rock pressure versus fluid pressure as a controlling influence on mineral stability: An example from New Mexico: American Mineralogist, v. 75, p. 1043–1058.
Holland, T. J. B., 1988, Preliminary phase relations involving glauconite and applications to high pressure petrology: Heat capacity and thermodynamic data: Contributions to Mineralogy and Petrology, v. 99, p. 134–142.
Hower, John, Eslinger, E., Hower, M. E., and Perry, E. A., 1976, Mechanism of burial metamorphism of argillaceous sediment 1. Mineralogical and chemical evidence: Geological Society of America Bulletin, v. 87, p. 725–737.
Huang, W. L., Bassett, W. A., and Wu, T.-C., 1994, Dehydration and hydration of montmorillonite at elevated temperatures and pressures monitored using synchrotron radiation: American Mineralogist, v. 79, p. 683–691.
Jam, L. P., Dickey, P. A., and Eysteinn, T., 1969, Subsurface temperatures in South Louisiana: American Association of Petroleum Geologists Bulletin, v. 53, p. 2141–2149.
Johnson, J. W., and Norton, D., 1991, Critical phenomena in hydrothermal systems: State, thermodynamic, electrostatic, and transport properties of $H_2O$ in the critical region.: American Journal of Science, v. 291, p. 541–648.
Johnson, J. W., Oelkers, E. H., and Helgeson, H. C., 1992, SUPCRT92: Software package for calculating the standard molal thermodynamic properties of minerals, gases, aqueous species, and reactions among them as functions of temperature and pressure: Computers and Geosciences,v. 18, p. 899–947.
Khitarov, N. I., and Pugin, V. A., 1966, Behavior of montmorillonite under elevated temperatures and pressures: Geokhimiya, v. 7, p. 790–795.
Koster van Groos, A. F. and Guggenheim, S.,1984, The effect of pressure on the dehydration reaction of interlayer water in Na-montmorillonite: American Mineralogist, v. 69, p. 872–879.
———— 1986, Dehydration of K-exchanged montmorillonite at elevated temperatures and pressures: Clays & Clay Minerals, v. 34, p. 281–286.
———— 1987, Dehydration of a Ca- and Mg-exchanged montmorillonite SWy-1 at elevated pressures: American Mineralogist, v. 72, p. 259–278.
Magara, Kinji, 1975, Reevaluation of montmorillonite dehydration as cause of abnormal pressure and hydrocarbon migration: American Association of Petroleum Geologists Bulletin, v. 59, p. 202–302.

Maier, C. G., and Kelley, K. K. (1932) An equation for the representation of high temperature heat content data: Journal of the American Chemical Society, v. 54,p. 3243–3246.
Parker, C. A., 1974, Geopressures and secondary porosity in the deep Jurassic of Mississippi: Transactions of the Gulf Coast Association of Geological Societies, v. 24, p. 69–80.
Perry, E. A., and Hower, J., 1972, Late-stage dehydration in deeply buried sediments: American Association of Petroleum Geologists Bulletin, v. 56, p. 2013–2021.
Pitzer, K. S., Peiper, J. C., and Busey, R. H., 1984, Thermodynamic properties of aqueous sodium chloride solutions: Journal of Physical Chemistry Reference Data, v. 13, p. 1–102.
Plumley, W. J., 1980, Abnormally high fluid pressure. Survey of some basic principles: American Association of Petroleum Geologists Bulletin, v. 64, p. 414–430.
Powers, M. C., 1967, Fluid release mechanisms in compacting marine mudrocks and their importance in oil exploration: American Association of Petroleum Geologists Bulletin, v. 51, p. 1240–1254.
Pytte, A. M., and Reynolds, R. C., 1988, The thermal transformation of smectite to illite, *in* Vaeser, N. D., and McCulloh, T. H., ed., Thermal Histories of Sedimentary Basins: New York, Springer Verlag, p. 133–140.
Ransom, Barbara and Helgeson, H. C., 1989, On the correlation of expandability with mineralogy and layering in mixed-layer clays: Clays & Clay Minerals, v. 37, p. 189–191.
———— 1993, Compositional end members and thermodynamic components of illite and dioctahedral aluminous smectite solid solutions: Clays & Clay Minerals, v. 41, p. 537–550.
———— 1994a, A chemical and thermodynamic model of dioctahedral 2:1 layer clay minerals in diagenetic processes: Regular solution representation of interlayer dehydration in smectite: American Journal of Science, v. 294, p. 449–484.
———— 1994b, Estimation of the molal heat capacities, entropies, and volumes of 2:1 clay minerals: Geochimica et Cosmochimica Acta, v. 58, p. 4537–4547.
Reynolds, R. C., 1992, X-ray diffractioin studies of illite/smectite from rocks: $<1$ μm randomly oriented powders and $<1$ μm oriented powder aggregates: The absence of laboratory artifacts: Clays & Clay Minerals, v. 40, p. 387–398.
Robie, R. A., Hemingway, B. S., and Fisher, J. R., 1978, Thermodynamic properties of minerals and related substances at 298.15 K and 1 bar ($10^5$ pascals) pressure and at higher temperatures: U. S. Geological Survey Bulletin 1452, 456 p.
Robinson, G. R. T., and Haas, J. L., 1983, Heat capacity, relative entropy, and calorimetric entropy of silicate minerals: An empirical method of prediction: American Mineralogist, v. 68, p. 541–553.
Stuart, C. A., 1970, Geopressures, Supplement to the Proceedings of the 2nd Symposium on Abnormal Fluid Pressures: Baton Rouge, Louisiana, Louisiana State University, p. 121.
Tardy, Yves, and Fritz, B., 1981, An ideal solid solution model for calculating solubility of clay minerals: Clay Minerals, v. 16, p. 361–373.
Vali, H., Hesse, R., and Martin, R., 1994, A TEM-based definition of 2:1 layer silicates and their interstratified constituents: American Mineralogist, v. 79, p. 644–653.
Velde, Bruce, and Vasseur, G., 1992, Estimation of the diagenetic smectite to illite transformation in time-temperature space: American Mineralogist, v. 77, p. 967–976.
Weaver, C. E., and Beck K. C., 1971, Clay water diagenesis during burial: How mud becomes gneiss, 96 p.